LA-12789-MS

UC-940
Issued: June 1994

Numerical Simulations in Support of the In Situ *Bioremediation Demonstration at Savannah River*

Bryan J. Travis
Nina D. Rosenberg

Los Alamos
NATIONAL LABORATORY
Los Alamos, New Mexico 87545

CONTENTS

TABLES

FIGURES

NUMERICAL SIMULATIONS IN SUPPORT OF THE *IN SITU* BIOREMEDIATION DEMONSTRATION AT SAVANNAH RIVER

by

Bryan J. Travis and Nina D. Rosenberg

ABSTRACT

This report assesses the performance of the *in situ* bioremediation technology demonstrated at the Savannah River Integrated Demonstration (SRID) site in 1992-1993. The goal of the technology demonstration was to stimulate naturally occurring methanotrophic bacteria at the SRID site with injection of methane, air and air-phase nutrients (nitrogen and phosphate) such that significant amounts of the chlorinated solvent present in the subsurface would be degraded. Our approach is based on site-specific numerical simulations using the TRAMP computer code. In this report, we discuss the interactions among the physical and biochemical processes involved in *in situ* bioremediation. We also investigate improvements to technology performance, make predictions regarding the performance of this technology over longer periods of time and at different sites, and compare *in situ* bioremediation with other remediation technologies.

EXECUTIVE SUMMARY

The Office of Technology Development (OTD) in the Department of Energy's (DOE) Office of Environmental Restoration and Waste Management is investigating new technologies for "better, faster, cheaper, safer" environmental remediation. A program at DOE's Savannah River site was designed to demonstrate innovative technologies for the remediation of nonarid sites contaminated with volatile organic compounds (VOCs). The Savannah River Integrated Demonstration (SRID) focused on two *in situ* remediation technologies aimed at remediating chlorinated solvent contamination in both the saturated and unsaturated (vadose) zones at a contaminated part of the Savannah River facility. The first demonstrated technology was *in situ* air stripping, a combination of air injection below the water table and vacuum extraction in the vadose zone, using a pair of horizontal wells. Later, a second technology, *in situ* bioremediation, was demonstrated using the same horizontal wells. The goal of the 428-day *in situ* bioremediation demonstration was to stimulate naturally occurring methanotrophic bacteria at the SRID site with injection of methane, air and air-phase nutrients (nitrogen and phosphate) such that significant amounts of the chlorinated solvents present in the subsurface would be degraded.

The purpose of this report is to assess the performance of the *in situ* bioremediation technology demonstrated at the SRID site. Our approach is to simulate the *in situ* bioremediation demonstration and then examine the simulation results to learn more about the interactions among the physical and biochemical processes involved.

We simulated removal of one of the main VOCs present at the site (trichloroethylene, TCE) during the *in situ* bioremediation demonstration at Savannah River using the computer code TRAMP. Our simulations indicate that the technology can be very effective in stimulating growth of methanotrophic bacteria over a wide area, and in biodegrading a significant amount of TCE *in situ*. In addition, these simulations demonstrated the usefulness and effectiveness of TRAMP for assessing field bioremediation tests.

Conclusions from our study regarding improvements to technology design include the following:

- A successful strategy should include pulsing of methane. It is important to remember, however, that the diffusivity of methane in air is about 10,000 times larger than in water. Therefore, pulsing in the unsaturated zone is less effective at saturated zone pulsing rates because discrete pulses of methane will not remain as spatially separated.
- Addition of nutrients significantly accelerates the biodegradation process by allowing the methanotroph population to grow rapidly. However, nutrient injection must be controlled to prevent explosive growth of bacteria near the injection wells, resulting in pore clogging and consumption of all the food substrate (methane) before it has a chance to spread throughout the system.
- If the methane and nutrients have the same transport properties (e.g., Henry's Law coefficient), then one should inject them together. If the methane and nutrients have significantly different transport properties, as in the Savannah River demonstration, then pulsing nutrients out of phase with the methane injection and systematically varying the phase lag would allow a larger region to be remediated efficiently and effectively.
- The goal in pulsing should be to maintain discrete pulses, without creating regions where methane and nutrient levels are too low (the bacteria will die) or too high (the bacteria will grow too much). To achieve this goal, several smaller wells may be more effective than a single pair of wells in some cases.

To compare the performance of *in situ* air stripping with *in situ* bioremediation, we ran our simulation of the field *in situ* bioremediation demonstration with the biokinetics part of the model turned off. All other features of the simulation were kept the same. Conclusions include the following:

- The total amount of TCE extracted or biodegraded by *in situ* bioremediation was 41% higher than the amount extracted by *in situ* air stripping — a significant enhancement of the removal rate of TCE.
- In addition to removing a greater total amount of TCE from the system, *in situ* bioremediation generally resulted in lower residual levels of TCE than *in situ* air stripping — in places by a factor of three to six lower.

Conclusions from our study regarding performance prediction include the following:

- Many of these same limitations of *in situ* air stripping apply to *in situ* bioremediation (e.g., long remediation times due mainly to VOCs in lower permeability clays), but *in situ* bioremediation can reduce remediation times and residual contaminant levels substantially.
- The main requirement for success is that methanotrophic bacteria exist at the site. Since methanotrophs are fairly common bacteria, this should not be a problem.
- *In situ* bioremediation with methanotrophs is not very dependent on site-specific factors at Savannah River, so the basic design of this technology should work at other sites.

- The details of technology implementation (e.g., injection strategy, well placement) which are key to its success, however, must be carefully evaluated for each new site. Site-specific scoping calculations will be necessary at each new site to determine the optimal number of wells, injection/extraction strategy, and so forth. Site-specific testing to obtain biokinetic rates to support these scoping calculations (i.e., laboratory tests on samples from the site which cover the range of nutrient, food and contaminant concentrations likely to be used or encountered) is strongly recommended.
- If VOC concentrations are much higher than at the SRID site, *in situ* bioremediation may not be effective. This is because at high concentrations, the contaminants can be poisonous to bacteria. In this case, *in situ* air stripping should be used to reduce the levels of VOCs to more moderate values before *in situ* bioremediation is attempted.

In situ air stripping was discussed in detail elsewhere and summarized in an appendix to this report; only the bioremediation aspects are considered here.

1. INTRODUCTION

Volatile organic compounds (VOCs) including chlorinated solvents such as trichloroethylene (C_2HCl_3, TCE) and perchloroethylene (C_2Cl_4, PCE) are among the most common contaminants in groundwater and soils. A common remediation approach has been to pump the contaminated groundwater to the surface where the water is treated to remove the contaminants. This pump-and-treat approach has been successful in containing contamination and removing much of the contaminant mass at many sites. It has been less successful at remediating sites to the low levels of residual contamination required by regulatory agencies. Moreover, cleanup efforts based on pump-and-treat are often costly and slow, and they do nothing to remediate VOCs in the vadose zone which may be a long-term source of groundwater contamination.

The Office of Technology Development (OTD) in the Department of Energy's (DOE) Office of Environmental Restoration and Waste Management is investigating new technologies for "better, faster, cheaper, safer" environmental remediation. A program at DOE's Savannah River site was designed to demonstrate innovative technologies for the remediation of sites contaminated with VOCs in nonarid environments. A similar project is underway at DOE's Hanford site to investigate technologies appropriate for remediating VOC contamination in arid environments.

The Savannah River Integrated Demonstration (SRID) focused on two *in situ* remediation technologies aimed at remediating contamination in both the groundwater and the vadose zone at a contaminated part of the Savannah River facility. The first demonstrated technology was *in situ* air stripping, a combination of air injection below the water table and vacuum extraction in the vadose zone, using a pair of horizontal wells. (Wells used for site remediation are typically vertical. Over the past few years, however, there has been an increased interest in horizontal wells for environmental remediation.) Later, a second technology, *in situ* bioremediation, was demonstrated using the same horizontal wells.

The purpose of this report is to assess the performance of the *in situ* bioremediation technology demonstrated at the SRID site, using numerical simulation as a tool. The approach is based on the construction of a model that approximates the field demonstration. The model is then used as a tool to estimate system performance at this site and to suggest how performance at different sites might vary (e.g., by extrapolating "lessons learned" from a single field demonstration). The performance of horizontal versus vertical wells and the performance of the SRID *in situ* air stripping demonstration are considered in separate reports (Birdsell et al. 1994, Robinson et al. 1994). Preliminary numerical calculations regarding the *in situ* bioremediation demonstration were presented in Travis et al. (1993).

2. SAVANNAH RIVER TECHNOLOGY DEMONSTRATION

2.1 Location

DOE's Savannah River facility is located in Aiken, South Carolina, near the South Carolina-Georgia border. The SRID site is part of a larger area that was used to process nuclear fuel and target elements for use in reactors. Degreasing operations were included at several stages of the processing. Chlorinated solvents, mainly TCE and PCE, were discharged to a seepage basin (M-Area Settling Basin) via a process sewer pipeline. In the early 1980s, inspections revealed that the process sewer line had extensive cracks, allowing solvents to leak into the subsurface environment. The SRID site is located at one of the areas where this sewer line is known to have leaked (Fig. 2.1).

2.2 Site Hydrogeology

The Savannah River site is underlain by sediments of the Atlantic Coastal Plain. The upper few hundred feet of these sediments consist of interbedded sands and clays that were deposited in shallow marine, lagoonal and fluvial environments. The local topography is relatively flat with an average surface elevation of ~360 feet above mean sea level.*

The sediments that underlie the site are heterogeneous, varying greatly in thickness and continuity across the site. A generalized description includes a sand unit and four major clay units. These clay units are known as the green clay, the tan clay, the 300-ft clay and the 325-ft clay. The 325-ft clay and the green clay are described as clays, whereas the tan clay and the 300-ft clay are described as clayey sands, sandy clays and interlayered clays and sands.

The water table lies at an elevation of ~230 ft, about 130 ft below the surface. A thin discontinuous aquitard (spatially undefined) exists at an elevation of ~225 ft separating a water table aquifer from a semiconfined aquifer. This semiconfined aquifer is separated from a confined aquifer by the green clay. See Fig. 2.2 and Eddy et al. (1991) and Eddy Dilek et al. (1993).

2.3 VOC Contamination

Sediment samples show the distribution of VOCs at the site to have been very uneven, generally concentrated in clay zones. The highest values for TCE and PCE in pre-*in situ* bioremediation demonstration (post-*in situ* air stripping demonstration) sediment samples were 6.3 and 1.6 μg/g (ppb), respectively.

The total subsurface inventory of VOCs at the site before the *in situ* bioremediation demonstration began is difficult to estimate. Based on sediment sampling data and interpolation calculations, Eddy Dilek et al. (1993) estimate an inventory of ~500 lbs of TCE and PCE for a volume about 300 ft by 250 ft wide centered over the old process sewer line before the *in situ* bioremediation demonstration. Monitoring data, however, indicate that over 12,000 lbs of TCE and PCE were removed through vapor extraction during the *in situ* bioremediation demonstration. The difference between the pretest inventory and the extracted quantity has been attributed to two causes: (1) contaminant from outside this volume was extracted during the demonstration and (2) initial inventory estimates are too low, because of losses during sampling. Additional details and discussion of the inventories are given in Eddy et al. (1991) and Eddy Dilek et al. (1993).

---

*Where original data are reported in English units, we have retained those units here.

2.4 Horizontal Wells

Two horizontal wells were used for the *in situ* air stripping and *in situ* bioremediation demonstrations (Looney et al. 1991). One well was installed below the water table and used for injection. This well is ~300 ft long and at an elevation of ~195 ft. A second well was installed in the vadose zone and used for vacuum extraction. This well is ~175 ft long and at an elevation of ~285 ft. The strike of the extraction well is ~35° to the strike of the injection well. Both wells are screened over most of their lengths and are subhorizontal, dipping toward greater depths at their terminal ends. Figure 2.2 shows the well locations at the SRID site.

2.5 *In Situ* Bioremediation Demonstration

At most sites, bacteria exist which can degrade a large variety of organic compounds, including many of the ones commonly found as groundwater and soil contaminants. In the case of chlorinated solvents, native bacteria cannot utilize these compounds directly as primary energy sources. There are families of bacteria (and other microorganisms such as fungi), however, which can cometabolize these solvents in the presence of a primary substrate (carbon source) such as methane (CH_4). This is possible because an enzyme the microorganisms produce to metabolize the primary substrate fortuitously transforms other compounds. For example, the methanotrophs (methane-oxidizing bacteria) produce methane monooxygenase (MMO) which initiates the oxidation of methane. MMO has a low specificity, however, and can initiate the oxidation of other compounds, including TCE. Because methanotrophs do not derive energy from the cometabolism of these chlorinated solvents (and in fact may even find the cometabolic by-products to be slightly poisonous), they require a supply of a substrate such as methane, along with oxygen and nutrients (nitrogen and phosphate), at appropriate concentrations to stimulate their growth.

The goal of the *in situ* bioremediation demonstration was to stimulate naturally occurring methanotrophic bacteria at the SRID site with injection of methane, air and air-phase nutrients (nitrogen and phosphate) such that significant amounts of chlorinated solvent present in the subsurface would be degraded. The demonstration began in late February 1992 and lasted about 420 days. A schematic of the processes involved in this technology is shown in Fig. 2.3.

Assessing the performance of the *in situ* bioremediation demonstration is difficult. With the *in situ* air stripping demonstration, there are uncertainties about contaminant distribution (see Section 2.3), but we do know that about 16,000 lbs of VOCs was removed from the subsurface. About 12,000 lbs of VOCs were removed during the *in situ* bioremediation demonstration, but the amount degraded *in situ* can not be directly measured. However, there are indirect measures, such as the increase in bacterial population counts, increase in chloride concentration and carbon dioxide, and other microbiological assays that indicate increased methanotrophic activity and metabolism of methane and mineralization of TCE. These suggest that anywhere from 500 to 2,000 lbs of TCE may have been biodegraded *in situ* (Hazen 1992b).

2.6 Modeling

Mathematical modeling of an *in situ* remediation demonstration is an attempt to capture the essential processes operating at a site and to study the interactions among those processes. A model is always an approximation to reality. A successful model will focus on the primary time and length scales, while averaging over smaller length and time scales. For a nonsimple model, numerical (rather than analytic) solutions are generally necessary. This entails specifying a grid that covers the region of interest. The size of the grid blocks in effect specifies the minimum length and time scales of the model. Processes operating on smaller scales are averaged. This is a reasonable thing to do since porous flow and transport are diffusive processes and will naturally tend to average over smaller scale features. Our models are based on the conservation

of mass and momentum. Constitutive equations are needed to complete the specifications of our model. These equations implicitly average out small scale dynamics. For example, the relationship between saturation and relative permeability is a constitutive equation that represents the sum total of pore scale movement of water in a small region of soil or rock as the total amount of water in that region varies.

Numerical models are based on conceptual models for how and where processes occur. In our model, fluid movement assumes the standard model described in many texts on porous media flow (Bear 1979). The biological kinetics component deserves some comment since this is a relatively new feature coupled to a flow and transport code and can be accomplished in a variety of ways. Figure 2.4 illustrates our assumptions. We assume that bacteria reside in the water phase, probably attached to soil grains, and that methane, oxygen and nutrient diffuse into the water phase from the air phase rapidly enough so that the air and water phase concentrations are in equilibrium. The diffusion time across a water film 100 microns thick is only about 10 seconds, which is considerably less than the residence time for gases in one meter sized numerical grid blocks, about 100-1000 seconds, so this appears to be a reasonable assumption. We assume that the TCE is dissolved in the water phase. The solubility of TCE in water (1100 ppm) is larger than any of the concentrations of TCE reported at the SRID site before the *in situ* bioremediation demonstration, so this is not an unreasonable assumption. Furthermore, if pockets of TCE existed as a separate phase, we would expect to see air phase densities at or near saturation and this is not the case. Numerical simulations of TCE leakage at the SRID site (Pruess 1993) suggest that significant amounts of TCE would exist as a NAPL (nonaqueous phase liquid) while leakage was occurring, but that after leakage stopped, TCE concentrations would gradually diminish to much lower levels due to vapor diffusion. Since some of the chemical species may diffuse into the grains of the soils and this is a slow process, we assume that a time lag exists before equilibrium can be established between fluid and solid phase concentrations. We also assume that the bacterial population can be represented by a single species whose properties represent an average of the probably heterogeneous microbial community. We assume that when a microbe dies, most but not all, of its internal nutrient store will be released quickly back into the environment for use by other bacteria. Our conceptual and mathematical model exists as a computer code called TRAMP (Travis 1993).

3. THE NUMERICAL MODEL

The computational model, TRAMP, has been developed jointly at Los Alamos National Laboratory (LANL) and HydroGeoChem Incorporated to support a number of field tests of *in situ* bioremediation (Bentley and Travis 1992, Travis 1993). TRAMP calculates the transport of air, water and dilute contaminants plus bacterial metabolism of substrates in porous media. TRAMP is capable of modeling both saturated and unsaturated flow and is not limited to the assumption of a steady flow field; all coupled flow and biokinetics codes of which we are aware (Molz et al. 1986, Widdowson et al. 1988, Celia et al. 1989, MacQuarrie et al. 1990, Rifai and Bedient 1990, Semprini and McCarty 1991, Kinzelbach et al. 1991, Wheeler et al. 1992) are limited to steady saturated flow fields. Compared to all of these other codes, TRAMP is broader and more sophisticated with respect to its capabilities. Most, for example, do not account for nutrient transport and cometabolism (e.g., BIOPLUME II) and only one of these other recent codes is 3-D (Wheeler et al. 1992).

TRAMP (TRAcr3d with Microbial Processes) is an extension of the TRACR3D code which simulates flow and transport of contaminants in porous media (Travis 1984, Travis and Birdsell 1991). A version of TRACR3D (TRACRN) has been qualified under the stringent software quality assurance requirements of the Yucca Mountain Project. TRAMP is an integration of TRACR3D with a sophisticated, relatively comprehensive biokinetics model developed by HydroGeoChem Incorporated (Bentley 1990). Both TRACR3D and TRAMP have been implemented on a number of computer systems, ranging from CRAYs to SUN workstations and they can be operated in 1-D, 2-D or 3-D mode.

TRAMP contains two sets of equations which are solved simultaneously. The first set includes the flow equations (mass conservation equations plus Darcy's Law for each phase velocity) for unsaturated/saturated flow of air and water in heterogeneous, anisotropic porous media. These are time-dependent, 3-D equations which are solved using an integrated finite difference, implicit time stepping algorithm.

The second set of equations in TRAMP includes six nonlinear, coupled time-dependent transport equations, one each for oxygen, two nutrients, two substrates (e.g., methane and TCE), and microbes. Both anaerobic and aerobic conditions are included. Monod kinetics are assumed. This coupled system is solved by an iterative finite difference algorithm. The biological activity model (Bentley and Travis 1992) is similar to that described by Widdowson et al. (1988) and Semprini and McCarty (1991). TRAMP is a general purpose code and therefore not all of its features may be needed at a specific site. The full equations used are given in Appendix A.

4. SITE SIMULATIONS

4.1 General Comments

Our goal in the first part of this study is to try to simulate the *in situ* bioremediation demonstration and then examine the simulation results to learn more about the interactions among the physical and biochemical processes involved. We then make estimates regarding the expected performance of this technology over longer times and at other sites, suggest possible improvements to technology design, and compare the performance of this technology with other remediation technologies.

It is important that simulation results be compared with laboratory and field data when possible. Agreement of simulated and field data does not *guarantee* that the model is a true representation of the field situation, but producing results that resemble what is observed in the field does provide some assurances. The model may not be correct in all details, but similarity in results suggests that the important aspects of the field situation have been captured by the model. (For an interesting and controversial discussion regarding validation of models, see Oreskes et al. 1994.)

4.2 Model Setup

Preliminary simulations of the *in situ* air stripping demonstration were performed using a full 3-D grid to estimate permeabilities. Here, however, we are restricting the domain to a 2-D cross-section. Figure 2.2 indicates the approximate location of the 2-D cross-sectional plane used in our simulations relative to the wells and the clay layers. This plane is approximately perpendicular to the direction of the horizontal wells. This plane is also close to many site monitoring wells, so that data from these wells can be used for comparison with the model results. The model domain (Fig. 4.1) includes the top 200 ft (60 m) of the subsurface and is 1,000 ft (300 m) in horizontal extent. From previous calculations, we expect that methane will spread horizontally for considerable distances. We are using a 1,000 ft horizontal extent to minimize the loss of methane from our model domain due to horizontal air flow.

The domain is divided into 1,560 rectangular grid cells. There are 40 rows of 1.5-m-thick grid cells. The horizontal grid spacing is variable. Grid cell widths are large on the left and right sides of the computational mesh and a uniform 3.7 m in the central 100 m. The bottom boundary is impermeable. The top boundary is open to the atmosphere, and pressure and concentrations are held fixed. The side boundaries are "free flow." This is a mathematical artifice, and works reasonably well, but not perfectly. Fluid pressure and contaminant concentrations at the side boundaries are approximately what they would be if the horizontal domain were infinite in extent and the fluid concentrations at the present boundary locations were monitored. This is much more realistic than having fixed-value side boundaries or impermeable side boundaries. Either one of those boundary conditions would create gradients at the sides that were either much too steep or much too shallow. The free flow boundary attempts to produce accurate gradients at the side boundaries.

The water table lies at 230 ft elevation (~130 ft below the surface). Initially the soil units below the water table are completely water saturated, but after injection begins, the upper part of the water table begins to desaturate. Earlier studies assumed uniform soil properties and relatively high permeabilities, and predicted a narrow cone of desaturation. Recently, Vlachopoulos and Kitinidis (1994) completed a more systematic analysis and found that the cone of desaturation can vary greatly in extent depending on the flow rates and the soil permeability. For our stratigraphy, with many clay lenses, we expect a low effective permeability, so that the region of desaturation should be quite wide, on the order of 100-200 m or so.

Properties of the soils needed for the air and water flow calculations are listed in Table 4.1.

Table 4.1. Hydrogeologic Values Used in Simulation

	325-ft Clay	300-ft Clay	Tan Clay	Sand
Horizontal permeability (darcy)	0.001	0.01	1	20
Vertical permeability (darcy)	0.0005	0.005	1	20
Porosity (%)	50	45	40	35
Initial saturation (%)	90	37	32	27
Coefficients for Brooks-Corey formulation for relative permeabilities and matric potentials as a function of water saturation:				
Bubbling pressure (in kPa)	40	30	25	10
Pore-size distribution index (0-1)	0.67	0.75	0.75	0.62
Irreducible saturation (%)	50	35	30	25

Initial values of concentrations for each chemical or biological species must be specified. For oxygen, a uniform concentration of 9.2 ppm in pore water is assumed. This represents equilibrium with air. The methanotroph population is assumed to be very small initially, on the order of 1 bacterium per cubic centimeter (1/cc) in the sands, 0.5/cc in the clayey sands, and 0.1/cc in the clays. These are consistent with measured values at the site. There is no methane in the domain initially. Two nutrients are used in these simulations — native and added. Nitrogen and phosphate are not treated separately since, presumably, bacteria will tend to use nitrogen and phosphate in constant proportion. Native nutrients are assumed present initially at low levels — 50 ppb in all soils.

The initial distribution of TCE is very heterogeneous. The distribution is based on the samples taken after the *in situ* air stripping demonstration (Eddy et al. 1991), while the magnitudes are based on what is needed to match the TCE concentrations observed at the extraction well during the *in situ* bioremediation demonstration. Figure 4.2 shows the initial distribution of TCE used in the model. The highest concentrations are in the clay units. Henry's law is applied to determine the partitioning between the air and liquid phases. Henry's law coefficients for the species in cgs units [(g/ml-air)/(g/ml-water)] are methane, 20, oxygen, 29, TCE, 0.37, and injected nutrient, 1.0. Molecular diffusivities of the species in the liquid phase are set to 10^{-5} cm^2/s for all except microbes, for which a value of 0 is assigned (no migration of bacteria). In the air phase, diffusivities are much larger. Values of 0.23 cm^2/s for methane, 0.1 cm^2/s for TCE, 0.14 cm^2/s for oxygen, and 0.10 cm^2/s for the nutrient are used.

The model allows methane, TCE, oxygen, and nutrient to sorb into the soil grains. This is a diffusional process and the rate of diffusion into or out of grains depends not only on the solid phase diffusivity (10^{-10} cm^2/s here) but also on the average soil grain sizes. We assume that the sand and clayey sand grains are roughly 0.5 mm in radius, and that the sandy clays and clay particles are about 0.25 mm in radius. The sorption coefficient, K_d, for methane on the soil grains has not been quantified experimentally. We use a value of 2.0 ml/g for K_d of TCE, consistent with measurements on Savannah River soils (Andrews 1994) and a small estimated value of 0.2 ml/g for methane.

Our simulation includes the following seven injection/extraction phases, which reflect the injection/extraction schedule of the field demonstration (Hazen 1992a, 1992b). The extraction well is turned on and pulls a constant 240 scfm (standard cubic feet per minute) (Phase 1). Extraction continues throughout the experiment. The injection well is then pressurized sufficiently to inject 200 scfm of air (Phase 2). During the next phase, 1% by volume of methane is added to the injection air stream (Phase 3). Later the methane is increased to 4% (Phase 4). This phase is followed by pure air injection (Phase 5), broken by an approximately one week period of injection of air with 2% by volume of methane and then with 1% methane, and pure air injection again. Next the methane content of the inflow is cycled, with 4% methane for eight hours, then just air for 40 hours (Phase 6). Finally, nutrient is added to the inflow stream at a constant concentration of 0.07% for N_2O and 0.007% for $TEPO_4$ (triethylphosphate) (Phase 7). This two-day cycle was repeated until shut down at 428 days. The total duration of the simulations is 475 days. The schedule for the different phases is shown in Table 4.2. Downtime due to maintenance and mechanical breakdown of equipment was ignored in the simulations. Influx of rain was also neglected.

Table 4.2. Injection/Extraction Schedule for Simulation

Phase	Time Initiated (day)
1. Extraction only	0
2. Air injection	21
3. 1% methane	56
4. 4% methane	161
5. Air only with a 2% pulse and a 1% pulse, one week each	240
6. Pulsing methane, 4%	300
7. Pulsing methane + continuous nutrient	341
Injection/extraction off	428

In addition to the TCE initially present in the model domain, TCE also enters the domain from a source outside the system. Based on the results of several simulations and field evidence for movement of TCE from a distant source (Looney et al. 1991), ~2 kg/day of TCE are estimated to be drawn into the model domain from outside due to the vacuum at the extraction well. We approximate this additional source by specifying a constant rate of injection of 2 kg/day of TCE

on the right boundary through a 10 ft vertical interval at a level slightly above the top of the tan clay (i.e., at ~90 ft depth) starting at day 150. This is marked in Fig. 4.1.

Parameter values used for the biokinetics submodel are listed in Table 4.3. These values are assumed to be constant in time and the subsurface temperature is assumed to be 20°C. Sources for these values include a series of field experiments conducted at Moffett Field, California (Roberts et al. 1990; Semprini et al. 1990, 1991; Semprini and McCarty 1991), laboratory tests performed by INEL on sandy soil from a contaminated region of the Snake River aquifer (Andrews et al. 1991), and in cases, our own judgment and experience. We considered the values for k_{CH4}, k_{TCE}, K_N, Y_{TCE}, k_d, F_N, and X to be adjustable. These parameters are, respectively, the maximum rate of methane and TCE utilization, the half saturation concentration for the nutrient, the microbial yield per unit of TCE consumed, the death rate of microbes, the amount of nutrient used per unit of bacteria, and the fraction of nutrient within a bacterium that is released after death. (All symbols are defined in Table A.1 in Appendix A.)

Although seven parameters are listed above as being adjustable, the situation is actually much more constrained; this was discussed in our preliminary simulations report (Travis et al. 1993). Two (k_{CH4} and k_{TCE}) are assumed equal since they both depend on the amount of MMO present. Y_{TCE} is expected to be very small and negative, or zero, because the bacteria may experience a slight poisoning effect from epoxides produced during TCE oxidation. We assume the nutrients to be nitrate and phosphate, in which case, F_N should be about 0.125, the fraction of a bacterium's weight that is nitrogen. X represents the fraction of nutrient in a bacterium that is readily available when the bacterium dies. It obviously must lie between 0 and 1. We assume a value of 0.9, near 1, but less than 1, to reflect our assumption that there is a time delay between bacterial death and availability of nutrient within the dead cell to the surrounding microbe community. The value of K_N is also limited. Since the bacteria appear to be moderately stressed, (i.e., nutrient starved), K_N should be considerably larger than the native nutrient concentration of 0.05 mg/l. K_N for other sites, however, has been determined to be about 0.20 mg/l. The death rate, k_d, of bacteria that we use, 1.5×10^{-6}/s, is in agreement with that determined at other sites. Although this could certainly vary, it is consistent with our efforts to match field data. The value used for k_{CH4} is obtained from matching the initial rapid rise phase of the bacterial populations when exposed to 1% methane. The value of I_{CH4}, which reflects the half-saturation at which methane inhibits TCE degradation, is not known with much certainty for this site. Our value is somewhat higher than that determined in other studies, for example Semprini and McCarty (1991), but was found necessary to match field data, and may simply reflect the fact that more than one microbial species are growing and probably attacking the TCE.

Table 4.3. Parameter Values Used in the Biokinetics Submodel

$C = 3 \times 10^{-11}$ g/ml	$M_o = 3 \times 10^{-5}$ g/ml
$Y_{CH4} = 5 \times 10^{-1}$ g (bacteria) /g (CH_4)	$Y_{TCE} = -1 \times 10^{-2}$ g (bacteria) /g (TCE)
$k_{CH4} = 1 \times 10^{-4}$/s	$k_{TCE} = 1 \times 10^{-4}$/s
$k_d = 1.5 \times 10^{-6}$/s	$k_C = 3 \times 10^{-7}$/s
$K_N = 100 \times 10^{-3}$ mg/l	$K_{CH4} = 0.2$ mg/l
$K_{TCE} = 1.0$ mg/l	$K_{O2} = 1.0$ mg/l
$I_{CH4} = 1.0$ mg/l	$F_{CH4} = 2.4$ g (O_2) / g (CH_4)
$F_{TCE} = 3.0$ g (O_2) / g (TCE)	$F_N = 0.125$ g (N) / g (M)
X = 0.9 g (N) / g (M)	$K_d^{TCE} = 2$ ml/g
$K_d^{CH4} = 0.2$ ml/g	

4.3 Simulations

The qualitative features of the simulation results are summarized in a series of color 2-D plots. Each plot is a "snapshot" of a chemical or biological component's spatial distribution at a selected time. In this section, we report detailed results from our "final run" only, but include comments regarding the large number of additional simulations which were made and which constitute a sensitivity analysis with regard to some parameters.

Figure 4.3 displays the methanotroph population count (log scale) at 100 days, 200 days, 300 days, 400 days, 430 days and 475 days. By 100 days, air plus 1% methane injection has stimulated bacterial growth to the 10^5 count range over a fairly broad region. The bacteria are following the methane trail, as expected (Fig. 4.4). By 200 days, the microbe population peak counts are down compared to 100 days, but the region of growth is more extensive, particularly in the left part of the domain. Although the methane is now at 4%, the bacteria have not shown a similar increase in numbers because they are limited by (native) nutrient. Growth in the right side of the domain is restricted to a narrow band along the original water table level and the area between the water table and the 300-ft clay. This is a region that has been desaturated by the injected airstream. Methane reaches this area, but not the region above. That area is primarily fresh air being sucked into the domain by the action of the extraction well.

At 300 days, the bacteria have died off considerably, especially in the injection region. During this time, air only (or air with occasional pulses of methane) are being applied and therefore the food supply for bacteria is greatly reduced (Fig. 4.4). There is still some methane in the left part of the domain. This is the region of highest bacterial population in the model at this time. By 400 days, the pulsing of methane and nutrients is well underway, and the bacteria are responding dramatically. There is intense growth in the vicinity of the injection well, with considerable activity in the vadose zone between the 300-ft clay and the tan clay as well. At 430 days, bacterial counts are beginning to drop off already in response to the general lack of methane. The methane injection has been off for a couple of days, and almost all the residual methane has been metabolized or diffused away. There is still sufficient nutrient to sustain bacterial growth, but there is no food substrate (i.e., methane). At 475 days, the injection and extraction wells are off, and the bacteria counts have dropped off by several orders of magnitude, reflecting the exponential death rate.

Figure 4.4 displays snapshots of the modeled methane distribution at 100, 200, 300, 400 and 430 days. Methane is spread for considerable distances horizontally by the injected air stream, especially in the left side of the domain. The lateral extent of the modeled region is 1,000 ft. Clearly, the modeled methane travels even farther than this, as evidenced by the exiting of methane through the domain boundaries. Near the surface, very low concentration levels occur during part of the demonstration and for limited time intervals. The 325-ft and 300-ft clays are very effective at restricting vertical flow. The 200-day picture shows high concentrations (3-4%) over a large lateral extent between the 300-ft clay and the injection well level. This level appears to be high enough to exceed the ability of the bacteria to metabolize it. At other times, methane is at much lower concentrations or near-zero due to microbial metabolism. On the right side, some methane tends to accumulate along the boundary between air flowing in through the side due to the suction of the extraction well and the methane-laden injected air which is rising and following an elliptical path toward the extraction well. At 430 days, methane is virtually absent, due primarily to the fact that the injection ended at 428 days, and bacteria have consumed any residual methane left in the soil. Also, during pulsing only 1/6 the amount of methane injected during the constant injection phase is being added, so average methane injected is only about 2/3% (4% * 1/6 = 2/3%).

Figure 4.5 displays TCE concentration fields (in the water phase) at 100, 200, 300, 400 and 430 days. These are not very dramatic images because of the scale; the maximum is set by the highest concentrations in the clay zones. It is clear that there is a gradual reduction of TCE

throughout the domain except for the clays. However, the clays near the injection well are actually being desaturated by the injected air pressure (1-2 atmospheres overpressure) to a sufficient degree to allow removal of TCE. The distant source of TCE is apparent on the right-hand side of the domain as the stream of TCE entering a little below the level of the extraction well. At 430 days, shortly after the demonstration has ended, there is a slight rebound of TCE due to slow desorption from clay grains.

Figure 4.6 also displays TCE water concentrations but at a reduced scale. Now it is easier to see regions that have been cleared of TCE, particularly in the sands, and in the clay lenses near the injection point. The influx of TCE on the right from a distant source prevents that area from being remediated to very low levels. The contaminated region at the bottom of the domain is not remediated in the model because injected air cannot reach that area; a hard clay layer lies about 10 ft below the injection well and blocks most downward air flow.

Figures 4.7 and 4.8 contain color contour plots of native nutrient at 100, 200 and 300 days, and added nutrient at 400 and 430 days. It is clear that the native nutrient is exhausted rapidly during the first 100 days when the bacteria experience their initial burst of growth. At 200 days, the nutrient supply is almost exhausted (at least in the region where methane is present), and bacterial growth is inhibited despite the fact that methane is present. At 300 days, there is a slight recovery of native nutrient due to release of nutrients from bacteria that died after the initial peak growth. At 400 days, the added nutrient is present in the inflow stream and has spread vertically and laterally for a considerable distance. Much of the nutrient however is in the vicinity of the injection well. The nutrient has a fairly low Henry's coefficient, meaning that it is quite soluble in water and thereby prevented from dispersing easily to great distances. Nevertheless, enough nutrient has spread beyond the injection point to stimulate growth over a wide area. At 430 days, its concentration is beginning to diminish because of continued microbial metabolism and shut-off of injection.

Figure 4.9 shows dissolved oxygen concentration at 100 days. Figure 4.10 shows water saturation at 200 days. By 200 days, a steady-state condition has been established with regard to the air flow and water distribution. Significant desaturation occurs, especially near the injection well. The water table is initially at a depth of 130 ft. By 200 days, water saturation levels have dropped from 100% initially to 50-60% in a cone with a radius of over 100 m, centered on the injection well, and about 50 ft deep at the well. Many of the clays are partially desaturated down to around 70-75% or so, opening up pore space and allowing TCE to escape. The supply of oxygen is generally more than sufficient for the microbial activity that occurs. Oxygen content in water is highest near the injection well as expected. Oxygen content only drops a few percent at most throughout the region. The microbial metabolic processes are not oxygen-limited.

The total amount of TCE extracted and biodegraded *in situ* in our simulation (at 428 days) is 1228 kg and 777 kg, respectively, for a total TCE removed from the subsurface of just over 2,000 kg (Fig. 4.11). The TCE is extracted at a nearly constant rate of 3.33 kg/day. The *in situ* biodegradation rate varies more, but averaged over the demonstration (from the point when methane injection begins) is ~2.1 kg/day. The ratio of TCE biodegraded to the mass of methane consumed by microbes is 0.19.

4.4 Comparison of Simulation Results and Field Data

Figure 4.12 shows the observed methane concentrations at the extraction well and the expected concentrations based on the helium tracer test. The simulated CH_4 profile (Fig. 4.13) looks very much like the expected CH_4 profile but arrival to plateau values is faster. Plateau values in the simulated case are higher, approximately 0.7% versus 0.6% during the 1% injected methane phase, and 2.9% versus 2.3% during the 4% phase. These differences are not unexpected and may simply reflect the considerably higher diffusivity in air of helium versus CH_4, which would

delay arrival of, and reduce peak amplitude. However, the model result is considerably larger than the observed CH_4 which only peaked at about 1% after approximately six months.

Figure 4.14 shows an initially rapid rise and decline of observed TCE in response to the start-up of the partial vacuum at the extraction well, followed by a gradual decrease. Over most of the demonstration, TCE is below 100 ppm at the extraction well, and varies between 50-75 ppm over the second half of the demonstration. Simulated TCE (Fig. 4.15) follows the same general trend but amplitudes are somewhat lower, especially in the very early phase, when concentration jumps from about 50 ppm to 100 ppm, then decreases back to 50-60 ppm, and decreases only very gradually. Late in the demonstration simulated TCE drops noticeably due to microbial action after nutrient is added to the inflow air stream.

The nearby vadose zone well, MHV-3, lies between the injection and extraction well and is close to the model cross-sectional plane (Fig. 2.2). Figure 4.16 shows the measured CH_4 concentrations at three depths in MHV-3 (95 ft, 70 ft, and 45 ft). In the deepest zone, peak CH_4 levels reach ~3.2% at ~240 days. The intermediate depth shows a narrower peak reaching to 2.8% and an average concentration of ~1.7% from 170 days to 230 days. Thereafter, concentration drops to ~0.5% until 310 days, then disappears until pulsing of CH_4 in the inflow air stream starts (around 360 days), and rises to ~0.5%. At the shallowest screen depth, CH_4 was not seen. Figure 4.17 shows the corresponding simulated CH_4 histories. A peak CH_4 concentration of about 3.7% is reached in the interval from 170 to 240 days; CH_4 then drops off to 0 briefly. There is a spike reaching to ~0.5% at 270 days which may correspond to the spike in Fig. 4.16 at about 290 days. Following a decrease to near-zero in both simulated and observed CH_4, there is then an increase to roughly 0.5% in both, but occurring somewhat earlier in the model. At the intermediate depth (which is the same depth as the extraction well), simulated CH_4 peaks at about 1%, which is lower than the observed peak of 3% and also somewhat later. Finally, at the shallowest depth in the simulation, methane only barely registers, reaching ~0.1% around 250 days. Perhaps the biggest difference between the field data and simulation results for MHV-3 is that the simulation results show CH_4 arriving during the 1% CH_4 injection phase whereas the field data do not.

Figures 4.18 and 4.19 compare observed and simulated methanotroph population counts at well MHT-4C, located between the injection and extraction wells, and below the original water table. There is an increase to $3x10^4$ cells/ml after 1% CH_4 is added to the injected air stream, followed by a second increase to approximately 10^6 cells/ml during the 4% CH_4 phase, then a drop-off of several orders of magnitude to a low at around 260 days. During the CH_4 pulsing and nutrient phase, population density increases quickly again to between 10^6 and 10^7 cells/ml, with a final drop-off after termination of the test. In the simulation (Fig. 4.18), microbe population density increases rapidly during the 1% CH_4 injection phase to roughly 10^6 cells/ml and then slowly decreases. Around 260 days, there is a further rapid decrease by another two orders of magnitude when CH_4 is absent from the injected air stream. Finally during the CH_4 pulsing and nutrient phase population counts jump to over 10^7 cells/ml until shutdown. The observed and simulated profiles at this location, (which is fairly typical of comparisons at other points as well) agree in the most general sense of increasing when CH_4 is injected and decreasing when CH_4 is absent, and the peak magnitudes are very roughly equivalent. The observed data show more variability (i.e., oscillations in values), probably revealing sensitivity to fluctuations in operations (maintenance time, pump malfunctions, etc.), and, possibly, interplay between several bacterial species and varieties not captured by the model.

The strongly 3-D nature of the site, as well as uncertainties in material properties, biokinetics, and so forth, precludes a closer match between model and observation. However, general trends do agree. The major difference is the absence of CH_4 at most monitoring wells during the 1% methane injection phase in the field data. The model shows that airborne nutrient is very effective at stimulating growth of bacteria over a wide area. These results also suggest that *in situ* bioremediation is effective in reducing contaminant levels to very low values (Fig. 4.20). At

360 days, nutrient is added to the inflow airstream. Microbe growth increases rapidly throughout much of the computational domain. MMO is available to degrade TCE. This is seen in the rapid drop of TCE from 120 ppb to about 20 ppb in Fig. 4.20. The location sampled is midway, both vertically and horizontally, between the injection and extraction wells. There is actually a rebound in TCE levels at this location to about 40 ppb by 400 days. This reflects a decrease in microbe population at this location due to a major decrease in methane concentration. There are two reasons for the drop in methane. First, during methane pulsing, less methane is being injected into the system, by a factor of six, than during the constant methane injection phases. Furthermore, the microbes near the injection well have increased dramatically in numbers, and are consuming most of the injected methane before it can spread very far. If nutrient and food substrate could be controlled and distributed more uniformly, the rebound effect should not occur and TCE levels would likely go lower.

5. DISCUSSION

In situ air stripping was discussed in detail elsewhere (Robinson et al. 1994). A brief summary is given in Appendix B. Only the bioremediation aspects of the *in situ* bioremediation technology are considered here.

5.1 Technology Optimization

Based on the simulation results discussed in the previous section, we now address the issue of technology optimization. What can be learned from our simulation work that can be used to improve the performance of *in situ* bioremediation? We focus here on the bioremediation aspects of the system. Optimization of *in situ* air stripping was discussed in detail in Robinson et al. (1994).

A successful strategy for *in situ* bioremediation should include pulsing of methane. A pulsing strategy makes sense for the following reason. While methane is present, bacteria grow; TCE degradation is inhibited during this phase by high methane concentrations. When methane is then temporarily removed, the bacteria population density will still be high and the bacterial MMO enzyme will be available to attack TCE; TCE degradation takes place in this phase. Under water-saturated conditions, pulsing of methane can be very effective. The diffusivity of methane is very small in water, so pulses of methane will remain separated spatially in the formation, allowing the pulsing strategy to work well. Methane diffusivity in the air phase, however, is about 10,000 times larger than in the water-saturated case. In the unsaturated case, this method is therefore less effective at the same pulsing rates because discrete pulses of methane will not remain as spatially separated. The methane pulses are very damped at some distance from the injection well.

A simple analysis can quantify this effect. Assume that methane pulses occur with a period of T seconds. Let the time from the end of one pulse to the beginning of the next be denoted by T_i. During one period, the center of the pulse will travel VT cm , where V is an average flow rate (in the air phase), and the edges of the pulses will diffuse out relative to the plume centers by approximately $\sqrt{2DT}$, where D is the diffusivity in air of methane. Pulses will be discrete and separate if $VT_i > 2\sqrt{2DT}$. Now $T = T_i+T_1$ where T_1 is the duration of a pulse, so that $V(T-T_1) > 2\sqrt{2DT}$ or, $V^2(T-T_1)^2 > 8DT$. If we write T_1 as a fraction x of T, then we get $VT^2 (1-x)^2 > 8DT$ or

$$T > 8D/V^2(1-x)^2.$$

This is the condition for pulses not to overlap during one cycle. If we require that pulses remain distinct over some total distance L_o, the analysis changes somewhat. Now we require that $VT_i > 2N\sqrt{2DT}$, where N is the number of cycles (L_o/VT). Our criterion for distinct pulses now becomes

$$VT_i > 2(L_o/VT)\sqrt{2DT}$$

or

$$T > \sqrt[3]{8L_o^2D/(V^4(1-x)^2)}.$$

For the SRID, we can make a very rough estimate for T if we assume L_o is approximately twice the distance between the injection and extraction wells (i.e., $L_o \approx 65$ m) and V is about 3 ft/day (10^{-3} cm/s, based on travel time for helium tracer peak concentration). In this case $T = 3.6 \times 10^6$s or about 42 days! (The minimum period for no overlap for one period is only about 12 days.) The estimates for V and L_o are very approximate, but in any case, T will be at least many days. The total methane injected will decrease greatly (compared to constant rate injection) since there

is a limit to how high a concentration can practically and safely be used to compensate for large periods. By contrast, for a water-saturated system, if other factors remained the same, T would be about two days (Fig. 5.1).

Next, we consider the role of nutrient injection. Nutrients were not added until late in the field demonstration. Our modeling (and the field data) suggest that addition of nutrients significantly accelerates the biodegradation process by allowing the methanotroph population to grow rapidly. Based on these results, we believe that if nutrients had been added earlier in the field demonstration, more dramatic results would likely have occurred. An additional simulation was made in which nutrients were added from the beginning of the demonstration to test the hypothesis that simply adding nutrients from the beginning of the demonstration would have resulted in more biodegradation of TCE. The results are somewhat surprising at first, in that less total TCE was removed than for the base case. After detailed examination of the simulation results, it was apparent why this was so. Addition of nutrients throughout the demonstration resulted in very high concentrations of bacteria in the vicinity of the injection well. The bacteria were in sufficient numbers to consume almost all of the methane injected, so that very little methane was being transported beyond the neighborhood (5-10 m) of the injection well. The bacteria reduced the levels of TCE near the injection site to extremely low levels, but they blocked the spread of the methane (i.e., the food) to more distant areas because of their high density. Supplying nutrients through the air phase as soluble gases appears to be an effective way to contact a large volume of soil relatively quickly. However, it is clear that nutrient injection must be controlled to prevent explosive growth of bacteria near the injection wells, resulting in pore clogging and consumption of all the food substrate (methane) before it has a chance to spread throughout the system.

How then should nutrients be added to the system? If in fact the nutrients and food substrate have the same transport properties (e.g., Henry's law coefficients and diffusivities), then one should inject them together. If the main food substrate (methane) and nutrients have significantly different transport properties, as in this demonstration, then pulsing nutrients out of phase with the methane injection and systematically varying the phase lag would allow a larger region to be remediated without problems of too much growth in the immediate vicinity of the injection well. A simple analysis can be made to quantify this operation. Let T, T_1 and V be defined as before, and let V_N be an average air phase speed for the nutrient substrate, Δt_{FN} the time lag between a food substrate pulse and the beginning of a nutrient pulse, and T_2 the duration of a nutrient pulse. It is assumed here that T, the period for injecting food, is equal to the period for nutrient injection. We expect also that $V_N = V/R_N$, where R_N is a total retardation of nutrients due to solubility and sorption. There are two cases to consider, $V_N < V$, and $V_N > V$, the former probably being more likely because many nutrients will be more soluble than methane. Figure 5.2 summarizes the analysis for the $V_N < V$ case.

The food substrate pulses (lines with slope V) occur at regular intervals and spread out in time due to diffusion (indicated by the dashed lines bounding the slope = V lines). The nutrient pulses are represented by lines of slope = V_N, which also broaden over time due to diffusion. The methane and nutrient pulses will interact at the locations d_0, d_1, d_2 and so forth given by

$$d_0 = VV_N(T-\Delta t_{FN})/(V-V_N)$$

and

$$d_m = d_0 + mV_NT, m \geq 1.$$

The intervals of intersection will also broaden in time due to diffusion. These widths are measured approximately by

$$I_{d_m} = V\left(VT_1 + V_NT_2 + m\left(\sqrt{2D_FT} + \sqrt{2D_NT}\right)\right) /(V-V_N).$$

For a given lag Δt_{FN} several separate locations d_m can be the locus of microbial growth due to the simultaneous arrival of both food and nutrient. After the pulses pass, the MMO enzyme will be disinhibited from attacking TCE. The locations of remediation, d_m, can be moved simply by changing the lag time Δt_{FN}, or (less practical for a given site and operation setup) the value of V_N. Care must be taken in choosing the initial concentrations of nutrient and food substrate in each pulse so that one or the other is not used up in the first pulse intersection or two. This depends both on the relative rates at which microbes can consume both and on the length of time a pulse intersection lasts. But qualitatively, nutrient pulses should be at relatively high concentration. For the (unlikely) case that $V_N > V$ (nutrient pulses travel faster than food pulses), a similar analysis is summarized in Fig. 5.3. The previous calculations for d_m and I_{dm} change slightly to

$$d_0 = VV_N\Delta t_{FN}/(V_N-V)$$

and

$$d_m = d_0 + mVV_NT/(V_N-V)$$

and

$$I_{d_m} = V_N\left(VT_1 + V_NT_2 + m\left(\sqrt{2D_FT} + \sqrt{2D_NT}\right)\right) /(V_N-V)$$

These analyses should be more accurate for low diffusivity systems, in particular, water-saturated ones. In high diffusivity systems, such as the vadose zone at the SRID, pulses will begin to lose their identity as discrete packages after only a few periods. This argues for using several wells, perhaps with lower flow rates, rather than a single pair of wells. Spacing between wells would be determined by the average flow rate between wells (which depends on permeability and injection/extraction rates) and the pulsing time interval, the period T, that is practical assuming two or at most three periods would be permitted between wells; that is, $L = N \cdot V \cdot T = 2VT$ where T is limited according to earlier analysis. Note that these analyses assume an equivalent uniform medium can be substituted for an actual site as a reasonable approximation.

In summary, it should be possible to design a strategy using pulses of nutrient and food substrate with variable lag between nutrient and food pulses to remediate a large area efficiently. The goal in pulsing should be to maintain discrete pulses, without creating regions where methane and nutrient levels are too low (the bacteria will die) or too high (the bacteria will grow too much and possibly clog pores). To achieve this goal, several wells may be more effective than a single pair of wells in some cases.

5.2 Comparison with *In Situ* Air Stripping

To compare the performance of *in situ* air stripping with *in situ* bioremediation, we ran the base case simulation discussed in Section 4 with the biokinetics part of the model turned off. All other features of the simulation (i.e., boundary conditions, initial conditions, injection/extraction schedules, geology) were kept the same. The amount of TCE extracted by *in situ* air stripping was 1424 kg during the first 428 days. When biokinetics is activated in the model, 1228 kg of TCE was extracted and 777 kg was biodegraded *in situ*. *In situ* air stripping removes slightly more TCE through vacuum extraction than is removed by vacuum extraction in the *in situ* bioremediation case due to removal of low levels of TCE along the main flow path by bacterial action.

The total amount of TCE removed (extracted and biodegraded) by *in situ* bioremediation was 2005 kg during the first 428 days. This is 41% higher than for *in situ* air stripping—a significant enhancement of the removal rate of TCE (Fig. 5.4). Our simulations show that in addition to removing a greater total amount of TCE from the system, *in situ* bioremediation generally results in lower residual levels of TCE than *in situ* air stripping. Figure 5.5 compares the TCE

concentration at a typical point for the two technologies. In the *in situ* bioremediation case, the bacteria have reduced the level of TCE by a factor of three to six below the level achieved by *in situ* air stripping alone.

5.3 Performance Predictions

The performance of *in situ* air stripping at the SRID over longer time periods was discussed in detail in Robinson et al. (1994). That study concluded that the TCE removal curve is very asymptotic. While remediating the sands is relatively easy, removing most of the TCE from the clays could take many years. Our results suggest that many of these same limitations apply to *in situ* bioremediation (e.g., long remediation times due mainly to VOCs in lower permeability clays), but that *in situ* bioremediation can reduce cleanup times substantially.

The main requirement for success is that methanotrophic bacteria exist at the site. Since methanotrophs are fairly common bacteria, this should not be a problem. *In situ* bioremediation with methanotrophs is not very dependent on site-specific factors at Savannah River, so there is no reason to believe that the basic design of this technology would not work at other sites. The details of technology implementation (e.g., injection strategy, well placement) which are key to its success, however, must be carefully evaluated for each new site. Site-specific scoping calculations will be necessary at each new site to determine the optimal number of wells, injection/extraction strategy, and so forth. Site-specific testing to obtain biokinetic rates to support these scoping calculations (i.e., laboratory tests on samples from the site which cover the range of nutrient, food and contaminant concentrations likely to be used or encountered) is suggested.

One caution is that if VOC concentrations are much higher than at the SRID, *in situ* bioremediation may not be effective. This is because at high concentrations, contaminants can be poisonous to bacteria. In this case, *in situ* air stripping should be used to reduce the levels of VOCs to more moderate values before *in situ* bioremediation is attempted.

6. CONCLUSIONS

We simulated removal of one of the main VOCs present at the site (TCE) during the *in situ* bioremediation demonstration at Savannah River using the computer code TRAMP. Our simulations indicate that the technology can be very effective in stimulating growth of methanotrophic bacteria over a wide area, and in biodegrading a significant amount of TCE *in situ*. In addition, these simulations demonstrated the usefulness and effectiveness of TRAMP for assessing field bioremediation tests.

Conclusions from our study regarding improvements to technology design include the following:

- A successful strategy should include pulsing of methane. It is important to remember, however, that the diffusivity of methane in air is about 10,000 times larger than in water. Therefore, pulsing in the unsaturated zone is less effective at saturated zone pulsing rates because discrete pulses of methane will not remain as spatially separated.
- Addition of nutrients significantly accelerates the biodegradation process by allowing the methanotroph population to grow rapidly. However, nutrient injection must be controlled to prevent explosive growth of bacteria near the injection wells, resulting in pore clogging and consumption of all the food substrate (methane) before it has a chance to spread throughout the system.
- If the methane and nutrients have the same transport properties (e.g., Henry's Law coefficient), then one should inject them together. If the methane and nutrients have significantly different transport properties, as in the Savannah River demonstration, then pulsing nutrients out of phase with the methane injection and systematically varying the phase lag would allow a larger region to be remediated efficiently and effectively.
- The goal in pulsing should be to maintain discrete pulses, without creating regions where methane and nutrient levels are too low (the bacteria will die) or too high (the bacteria will grow too much). To achieve this goal, several smaller wells may be more effective than a single pair of wells in some cases.

To compare the performance of *in situ* air stripping with *in situ* bioremediation, we ran our simulation of the field *in situ* bioremediation demonstration with the biokinetics part of the model turned off. All other features of the simulation were kept the same. Conclusions include the following:

- The total amount of TCE extracted or biodegraded by *in situ* bioremediation was 41% higher than the amount extracted by *in situ* air stripping—a significant enhancement of the removal rate of TCE.
- In addition to removing a greater total amount of TCE from the system, *in situ* bioremediation generally resulted in lower residual levels of TCE than *in situ* air stripping—in places by a factor of three to six lower.

Conclusions from our study regarding performance prediction include the following:

- Many of these same limitations of *in situ* air stripping apply to *in situ* bioremediation (e.g., long remediation times due mainly to VOCs in lower permeability clays), but *in situ* bioremediation can reduce remediation times and residual contaminant levels substantially.
- The main requirement for success is that methanotrophic bacteria exist at the site. Since methanotrophs are fairly common bacteria, this should not be a problem.

- *In situ* bioremediation with methanotrophs is not very dependent on site-specific factors at Savannah River, so the basic design of this technology should work at other sites.
- The details of technology implementation (e.g., injection strategy, well placement) which are key to its success, however, must be carefully evaluated for each new site. Site-specific scoping calculations will be necessary at each new site to determine the optimal number of wells, injection/extraction strategy, and so forth. Site-specific testing to obtain biokinetic rates to support these scoping calculations (i.e., laboratory tests on samples from the site which cover the range of nutrient, food and contaminant concentrations likely to be used or encountered) is strongly recommended.
- If VOC concentrations are much higher than at the SRID site, *in situ* bioremediation may not be effective. This is because at high concentrations, the contaminants can be poisonous to bacteria. In this case, *in situ* air stripping should be used to reduce the levels of VOCs to more moderate values before *in situ* bioremediation is attempted.

In situ air stripping was discussed in detail elsewhere (and briefly summarized in Appendix B); only the bioremediation aspects are considered here.

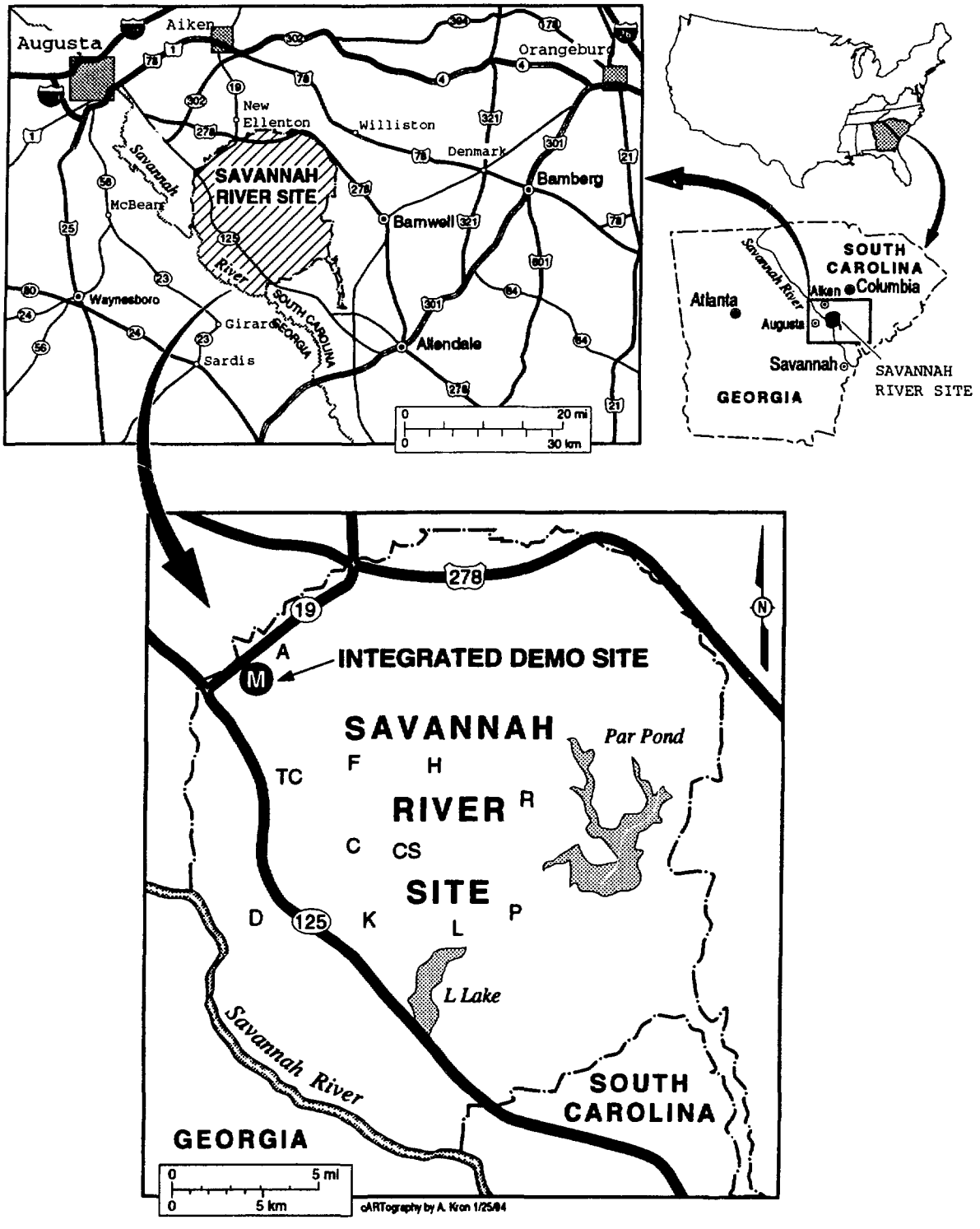

Fig. 2.1. Location of Savannah River facility and Integrated Demonstration site.

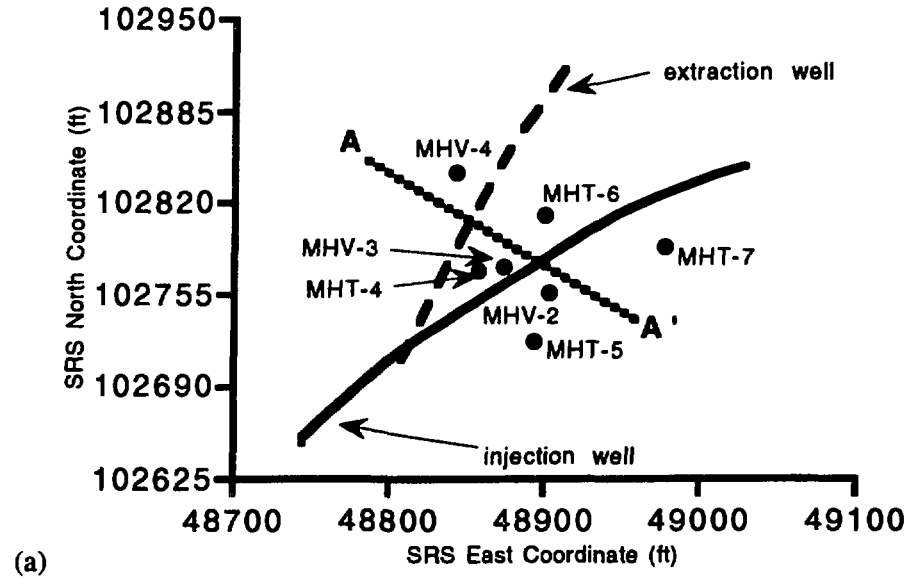

(a)

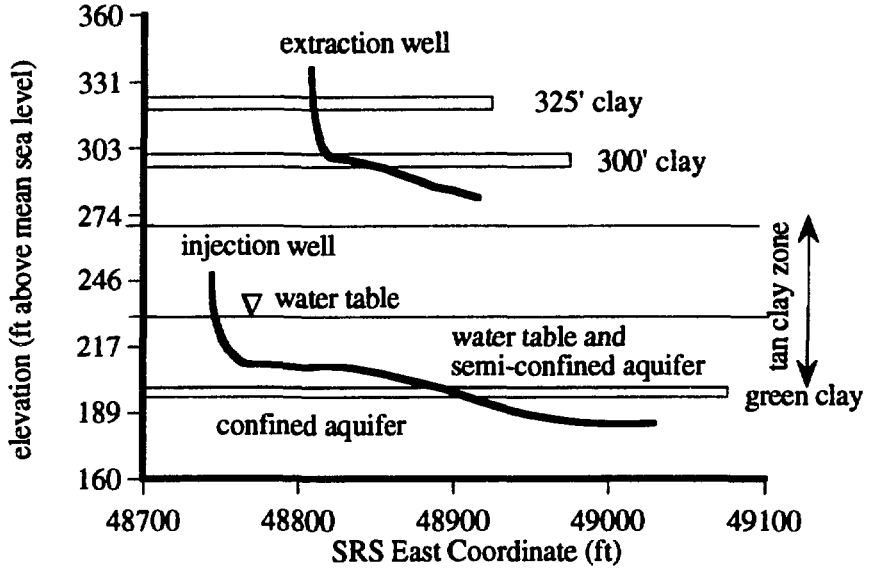

(b)

Fig. 2.2. Generalized hydrogeology and location of horizontal wells (a) map view, (b) cross-section. A-A' represents the 2-D cross-section modeled in our simulations.

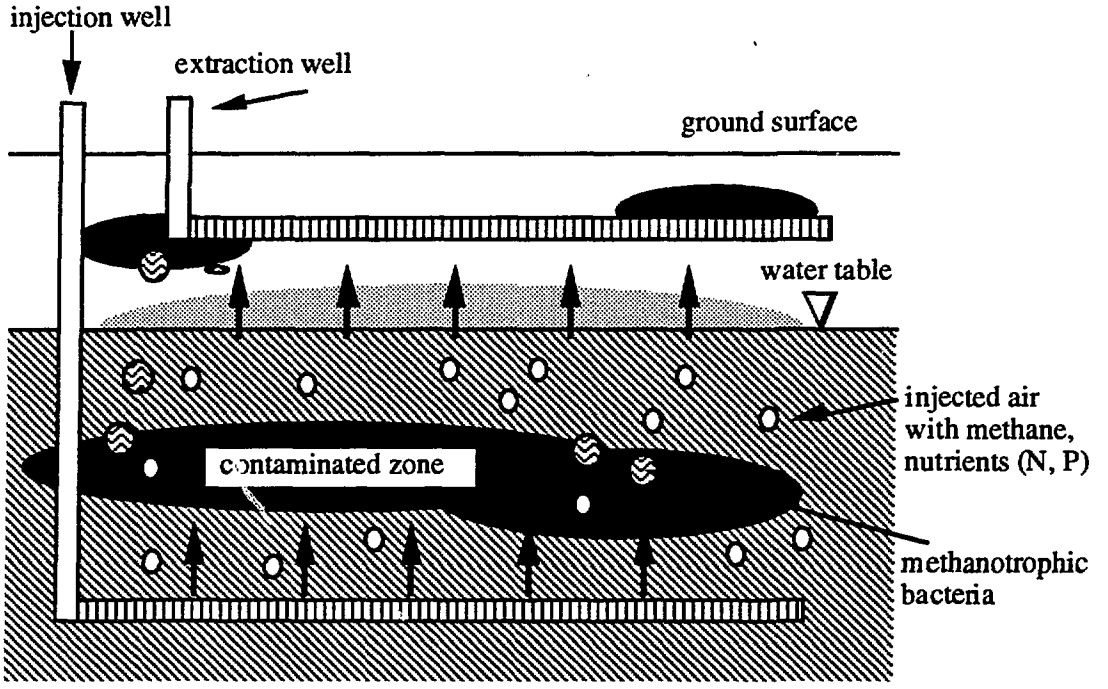

Fig. 2.3. Schematic of *in situ* bioremediation technology.

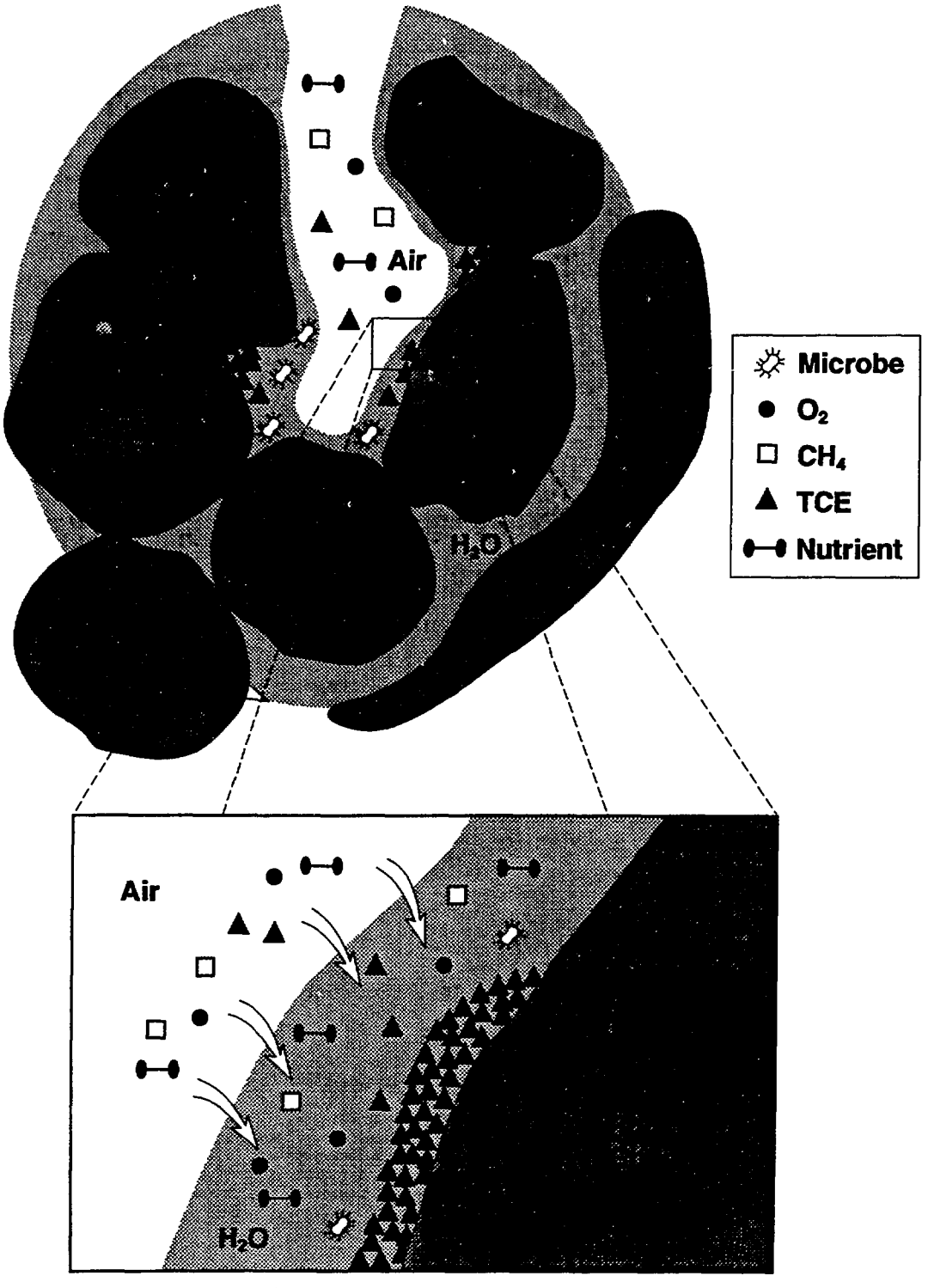

Fig. 2.4. Schematic illustration of bioremediation processes at the pore-scale.

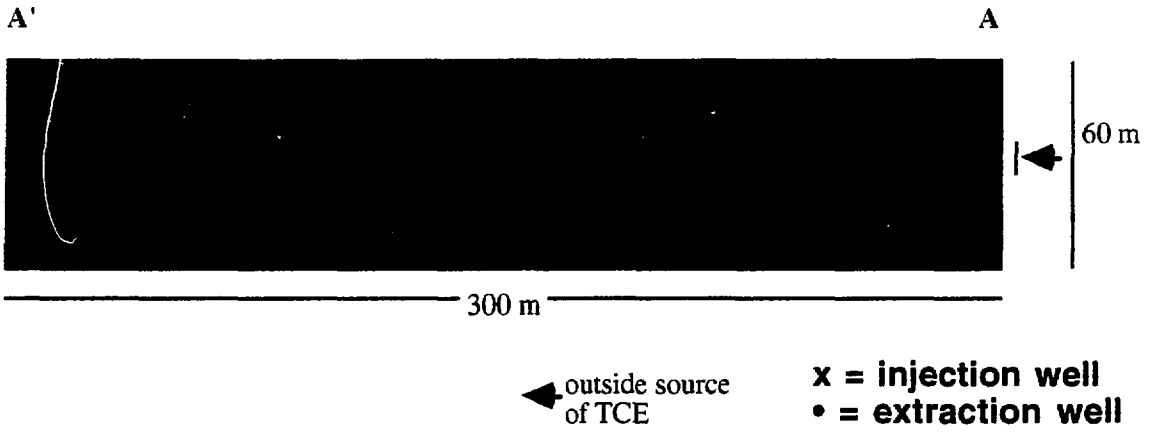

Fig. 4.1. Model domain. The colors represent different hydrologic units: purple = sand, blue = tan clay, green = sandy clay and red = clay.

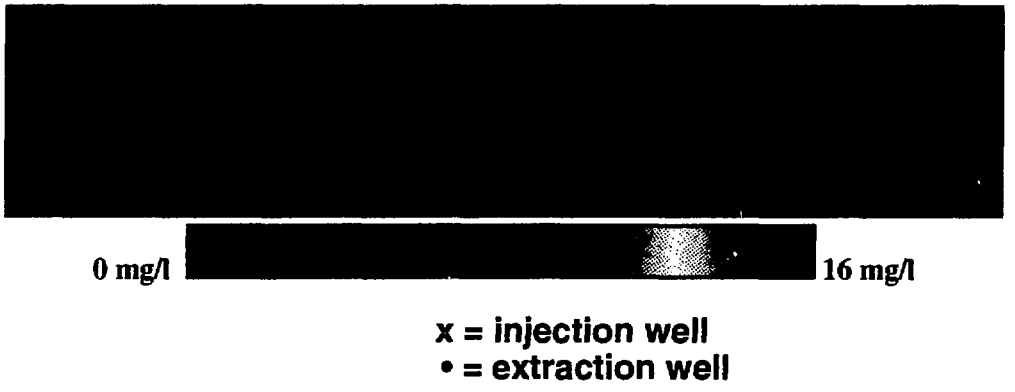

Fig. 4.2. Initial distribution of TCE in the model.

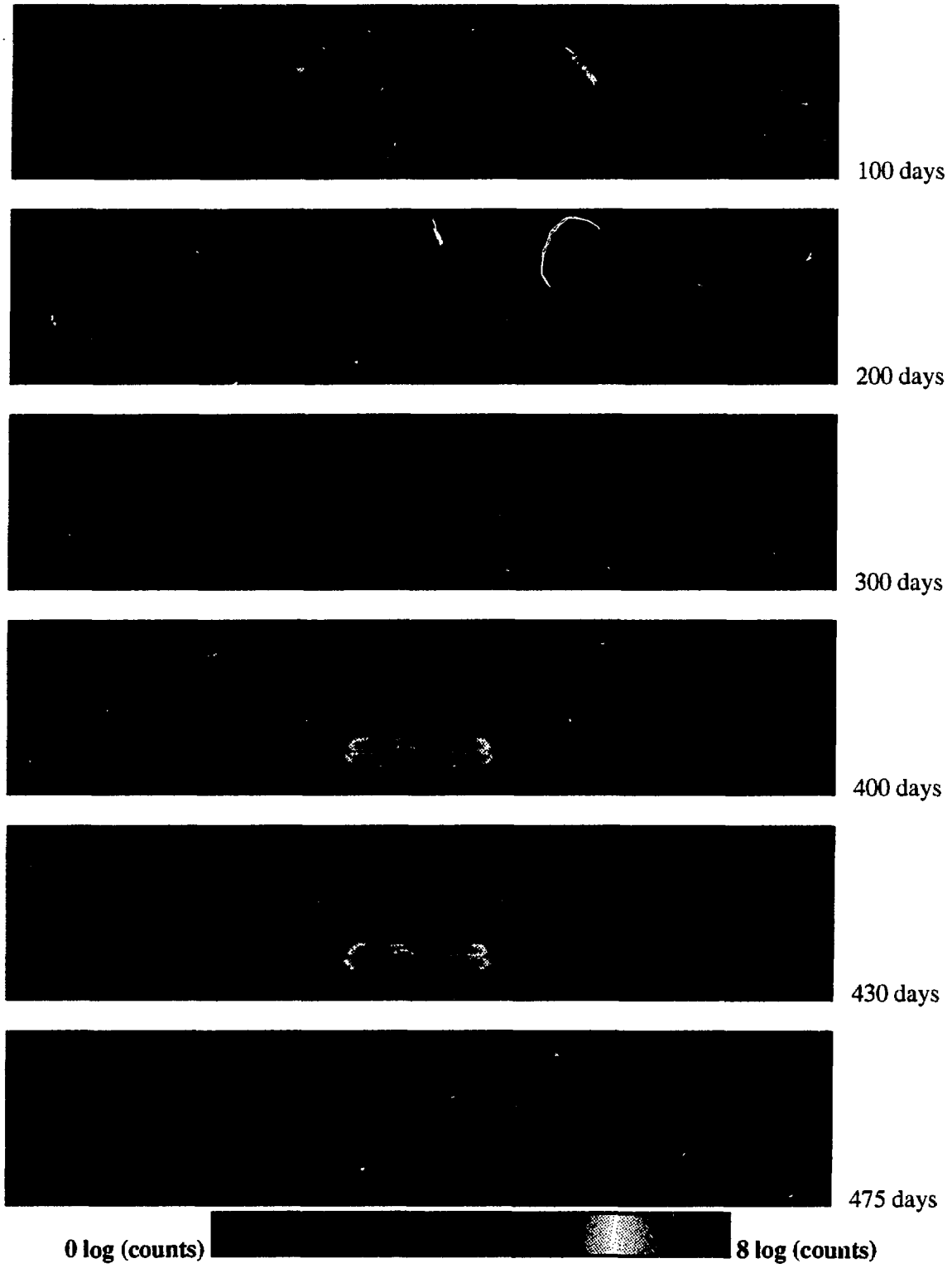

Fig. 4.3. Bacteria population distribution at selected times.

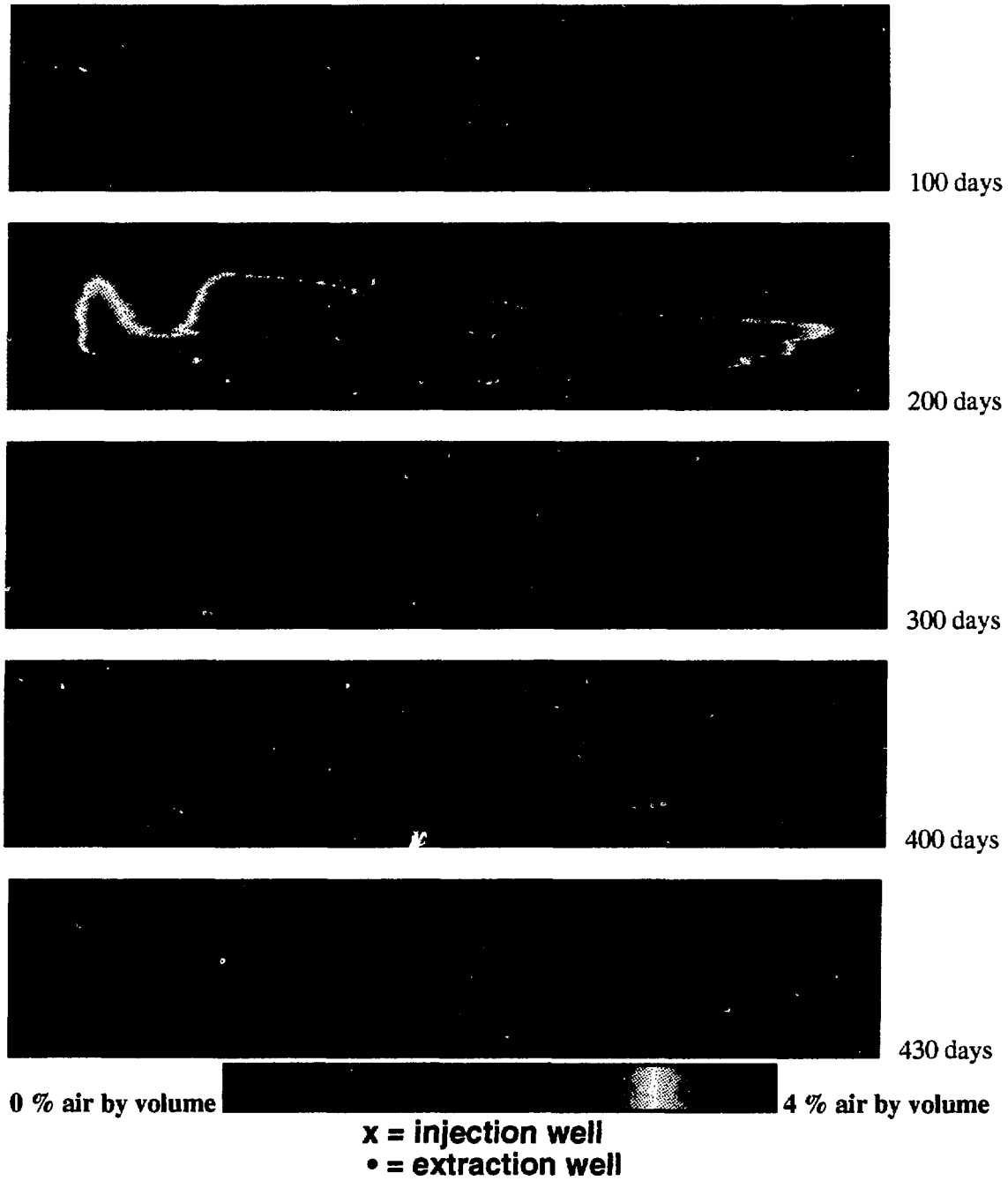

Fig. 4.4. Methane distribution at selected times.

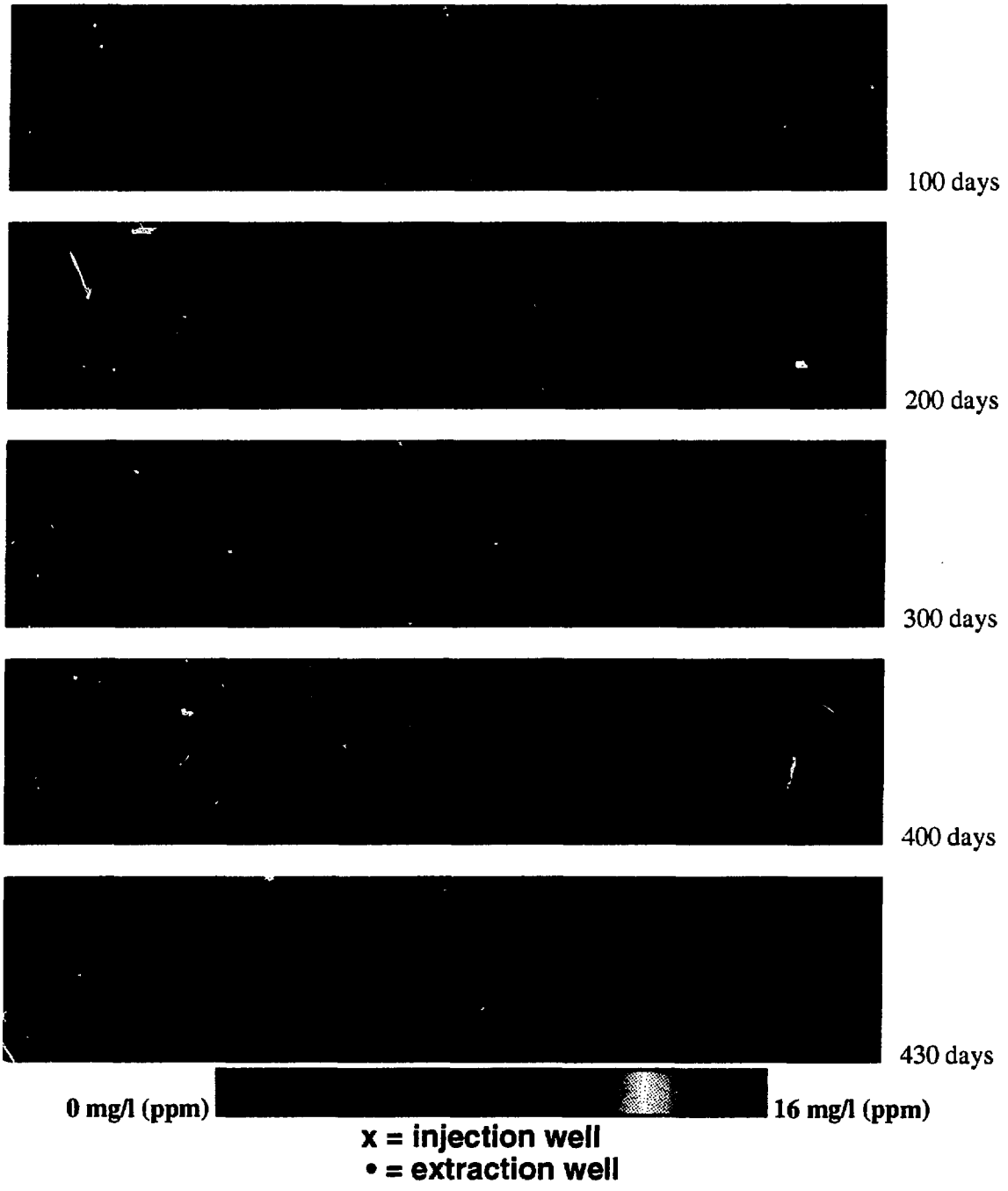

Fig. 4.5. TCE distribution at selected times.

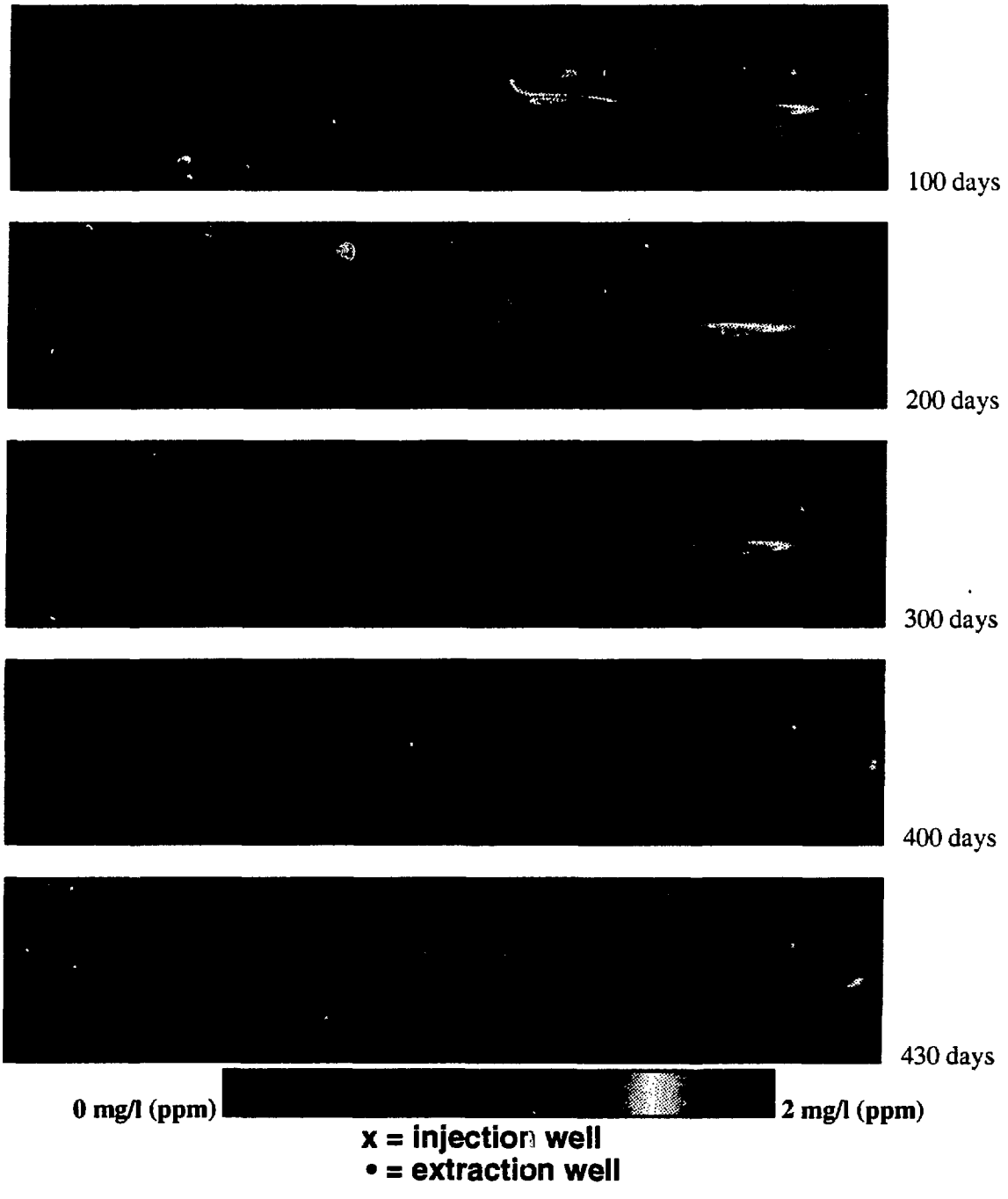

Fig. 4.6. TCE distribution at selected times, limited range scale.

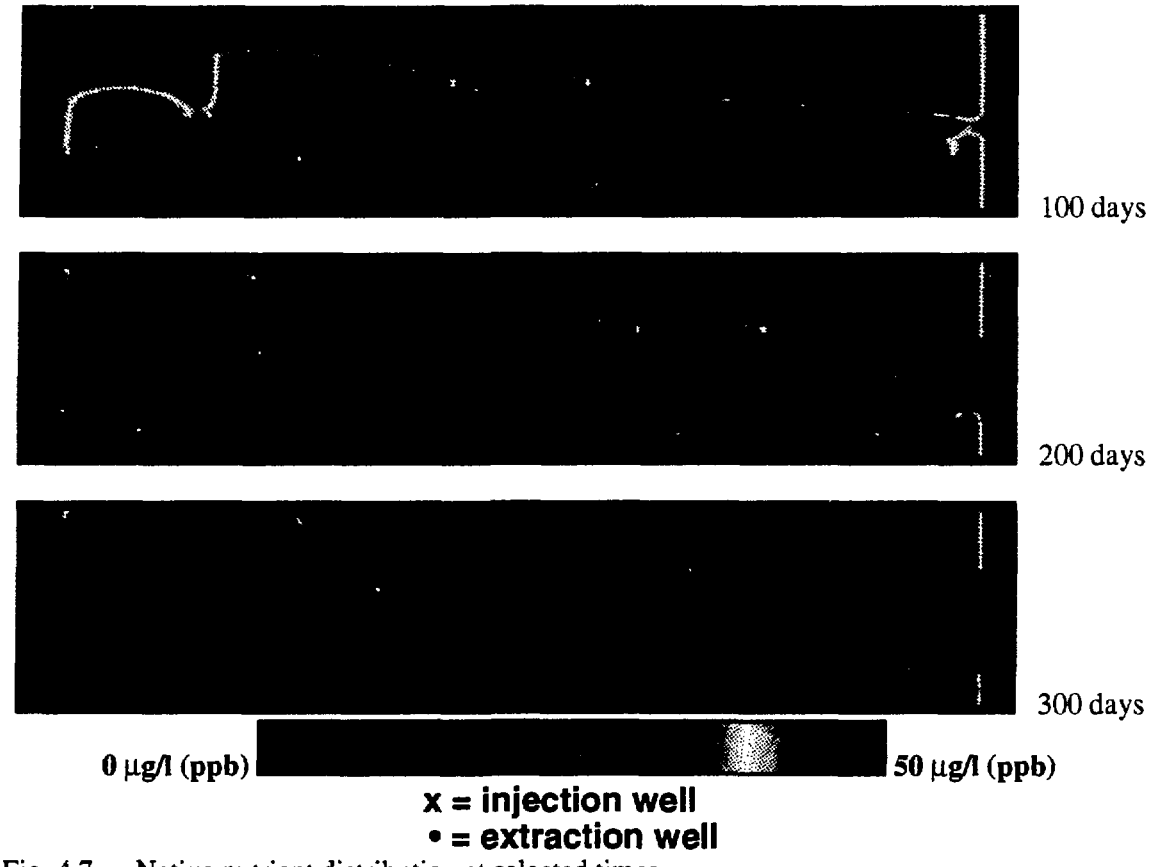

Fig. 4.7. Native nutrient distribution at selected times.

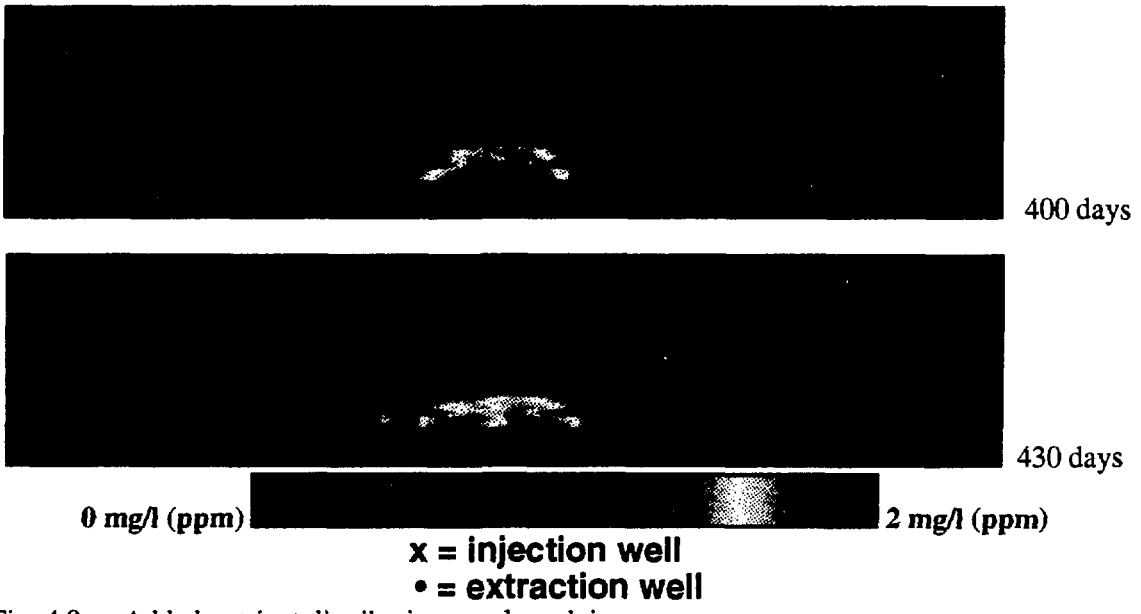

Fig. 4.8. Added nutrient distribution at selected times.

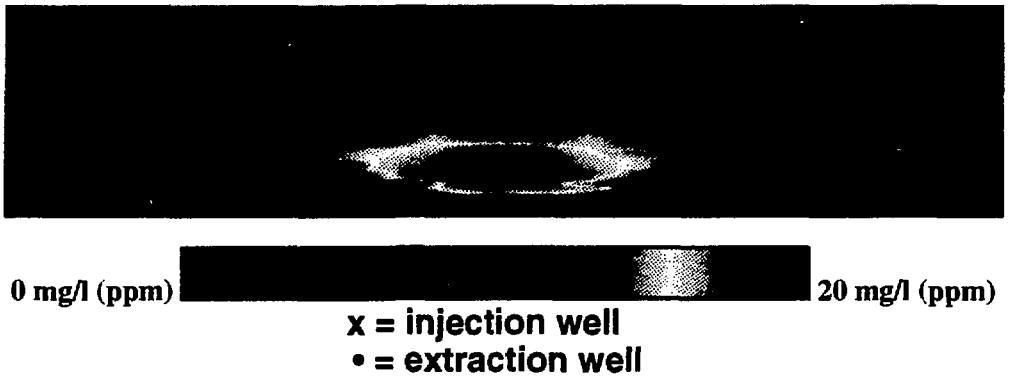

Fig. 4.9. Oxygen distribution at 100 days.

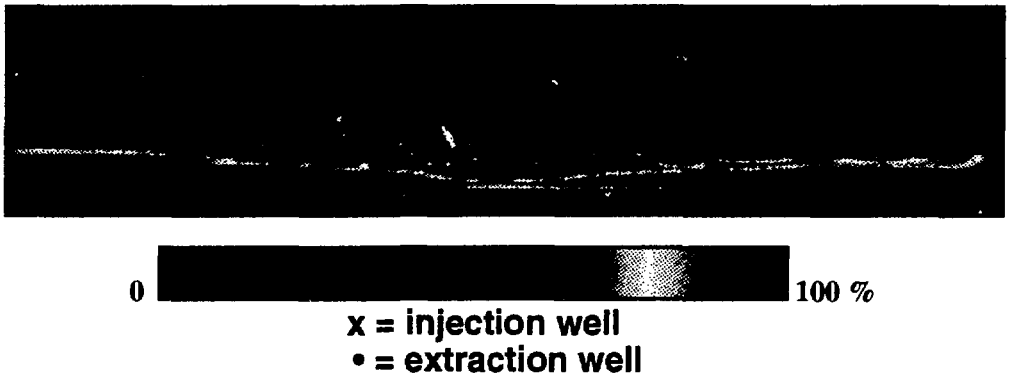

Figure 4.10. Water saturation at 200 days.

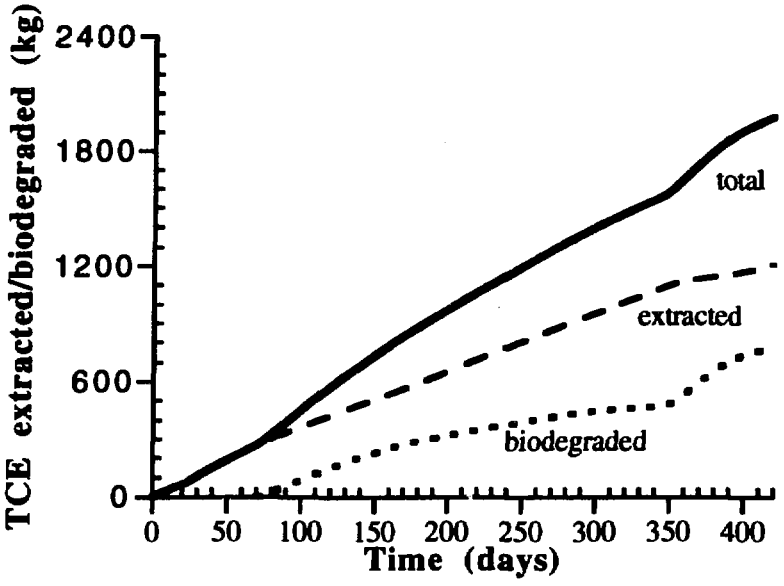

Fig. 4.11. TCE extracted/degraded vs. time for *in situ* bioremediation simulation.

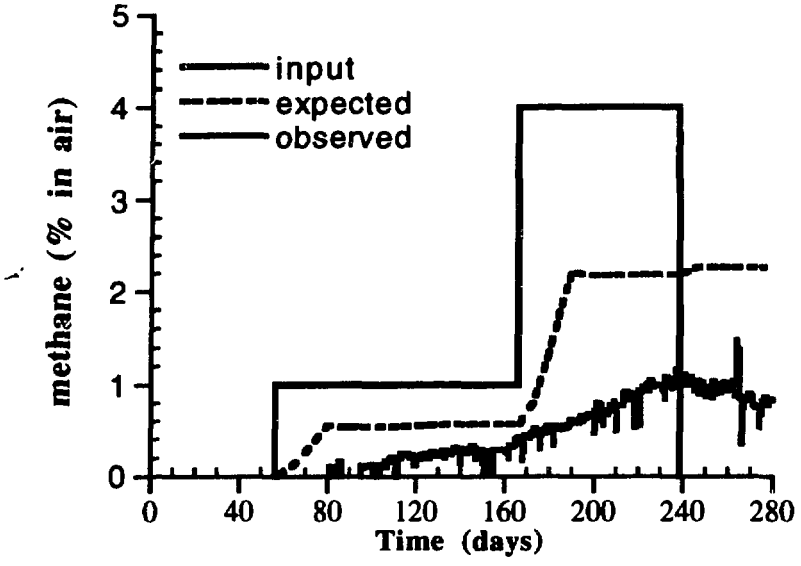

Fig. 4.12. Methane injected and methane at the extraction well vs. time (expected and observed). The expected methane levels are projections based on a helium tracer test.

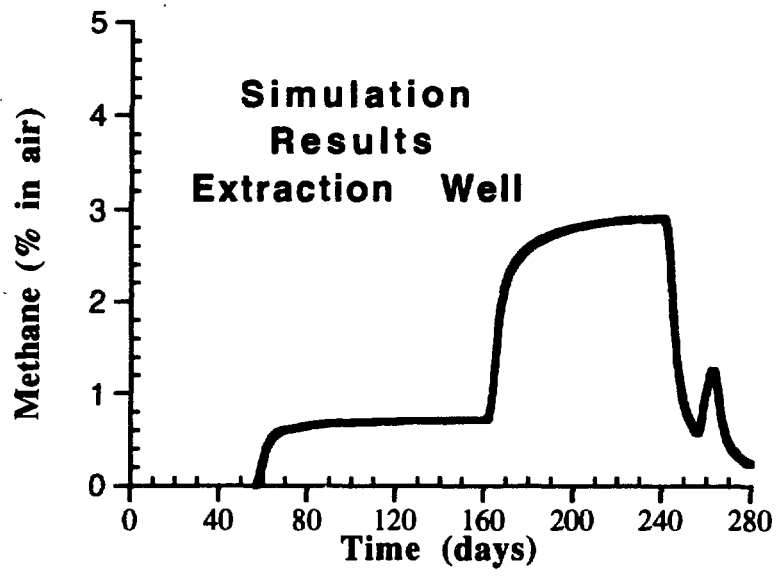

Fig. 4.13. Simulated methane concentration vs. time profile at the extraction well.

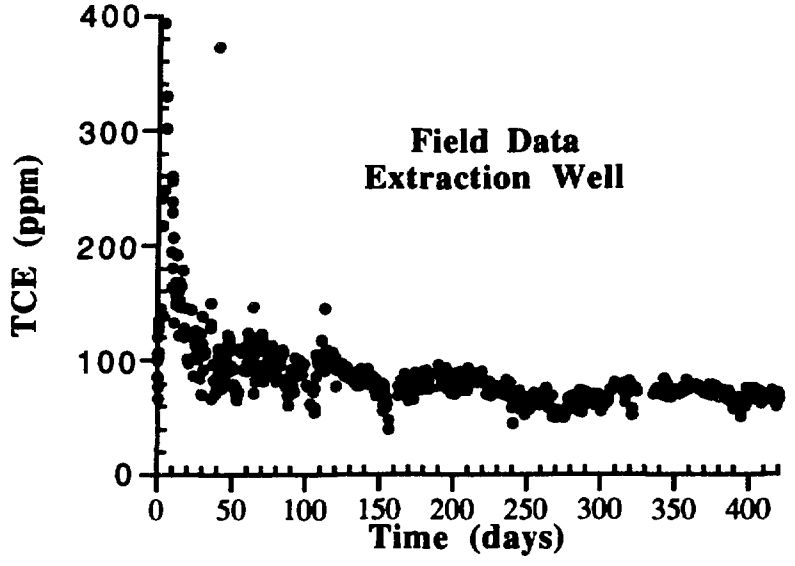

Fig. 4.14. Observed TCE concentration vs. time profile at the extraction well. Data from Hazen (1992b).

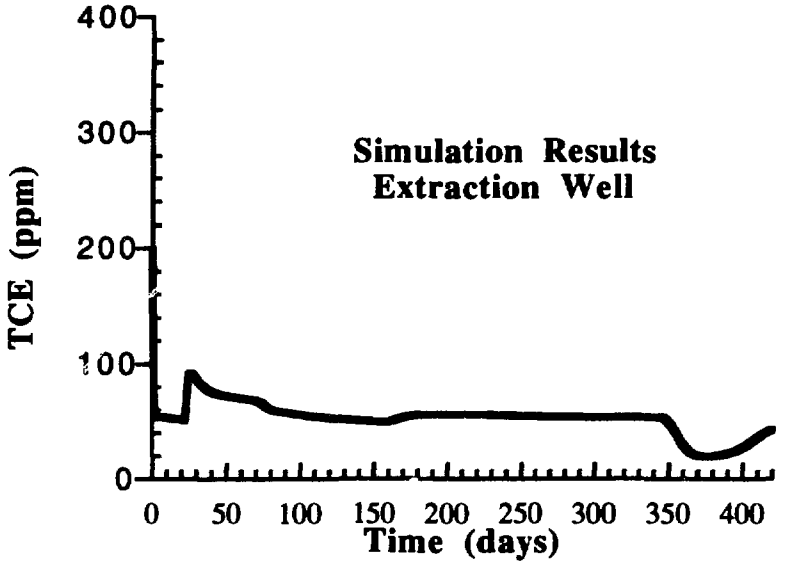

Fig. 4.15. Simulated TCE concentration vs. time profile at the extraction well.

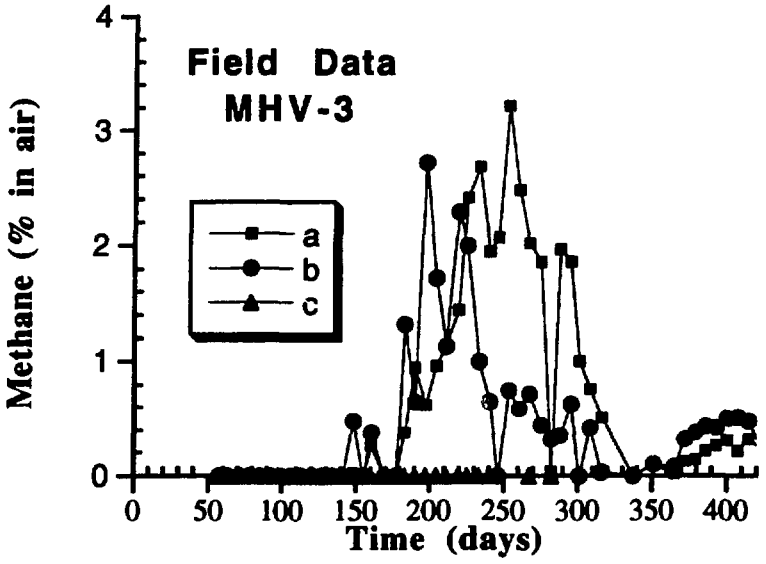

Fig. 4.16. Observed methane concentration vs. time profile at MHV-3. Data from Hazen (1992b).

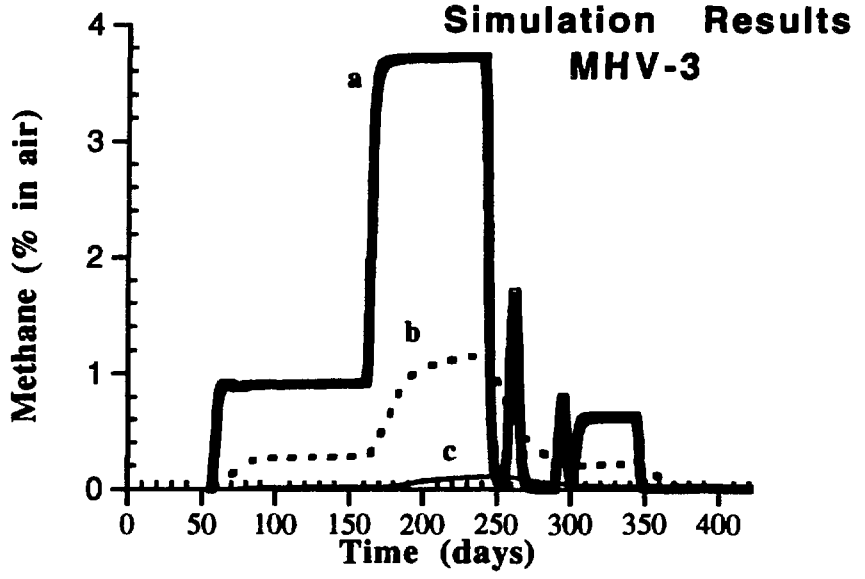

Fig. 4.17. Simulated methane concentration vs. time profile at MHV-3.

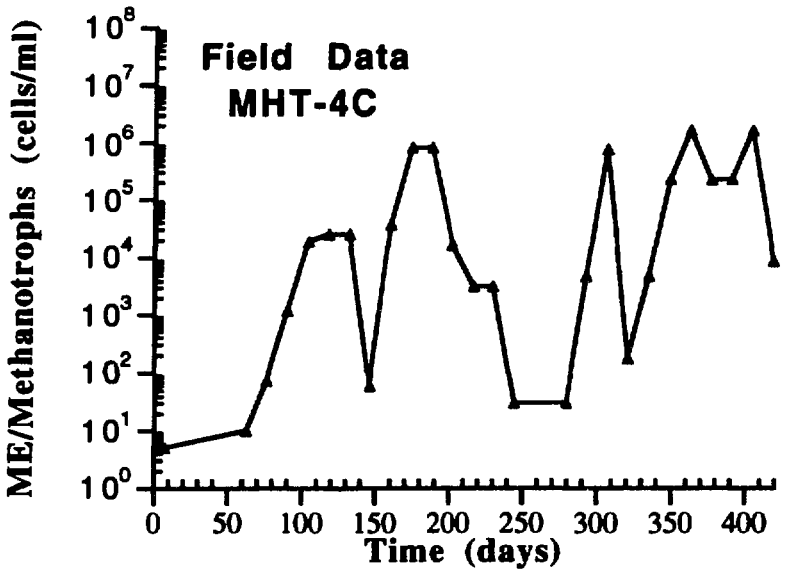

Fig. 4.18. Observed bacteria counts vs. time profile at MHT-4C. Data from Hazen (1992b).

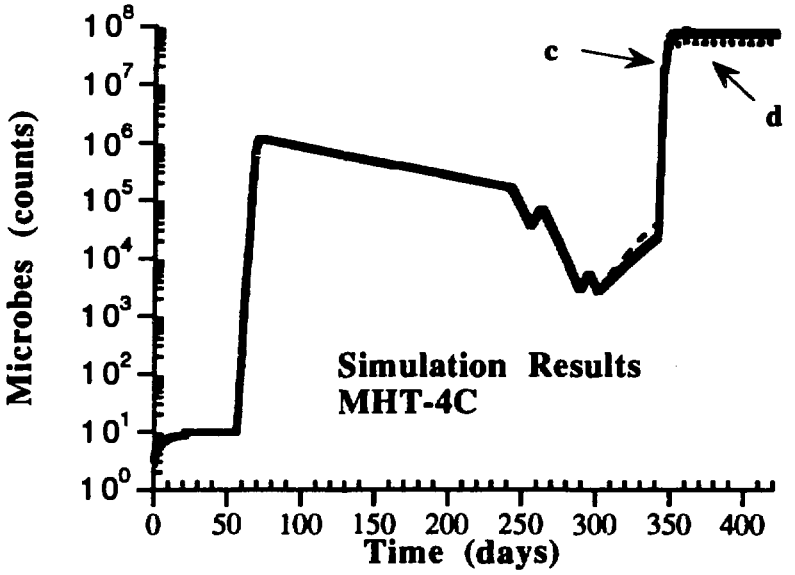

Fig. 4.19. Simulated bacteria counts vs. time profile at MHT-4C.

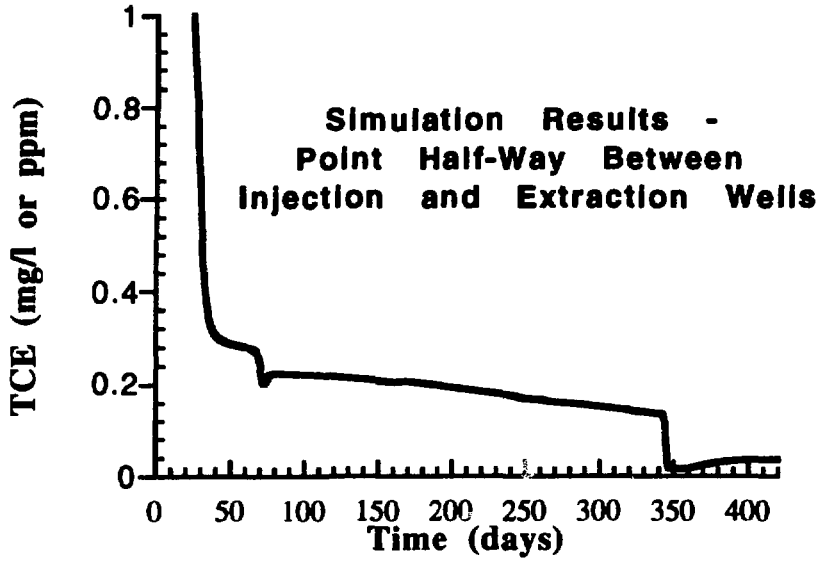

Fig. 4.20. Simulated TCE concentration vs. time profile at point half-way between injection and extraction wells.

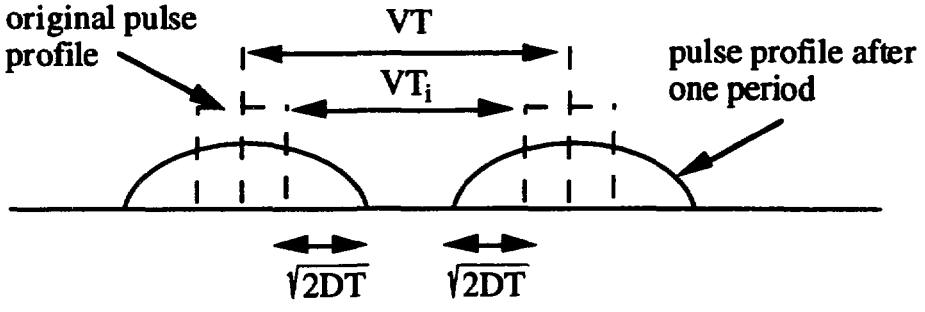

Fig. 5.1. Schematic illustrating separation of pulses and diffusion of original square wave pulses.

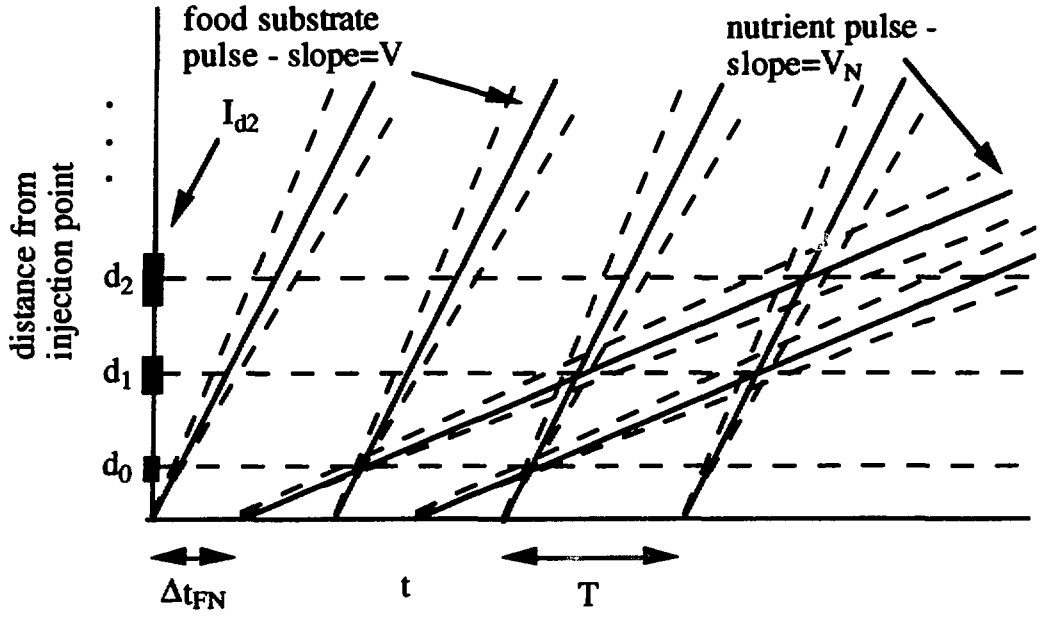

Fig. 5.2. Plot of food substrate pulse and nutrient pulse as a function of distance and time. Enhanced microbial growth and biodegradation will occur at the intersections of the nutrient (slope = V_N lines) and the food substrate pulses (slope = V lines) ($V_N < V$ case.)

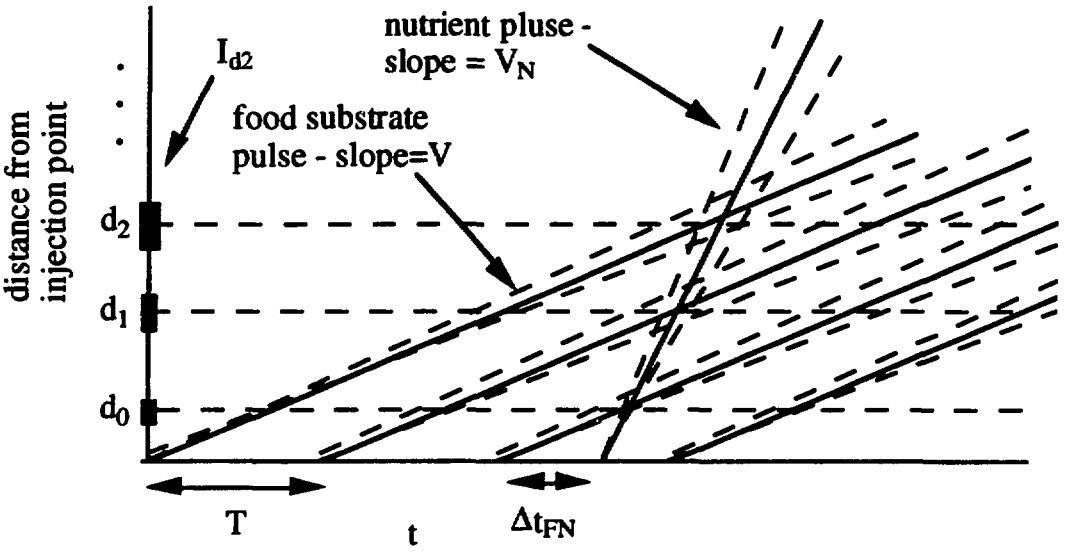

Fig. 5.3. Plot of food substrate pulse and nutrient pulse as a function of distance and time. Enhanced microbial growth and biodegradation will occur at the intersections of the nutrient (slope = V_N lines) and the food substrate pulses (slope = V lines) ($V < V_N$ case.)

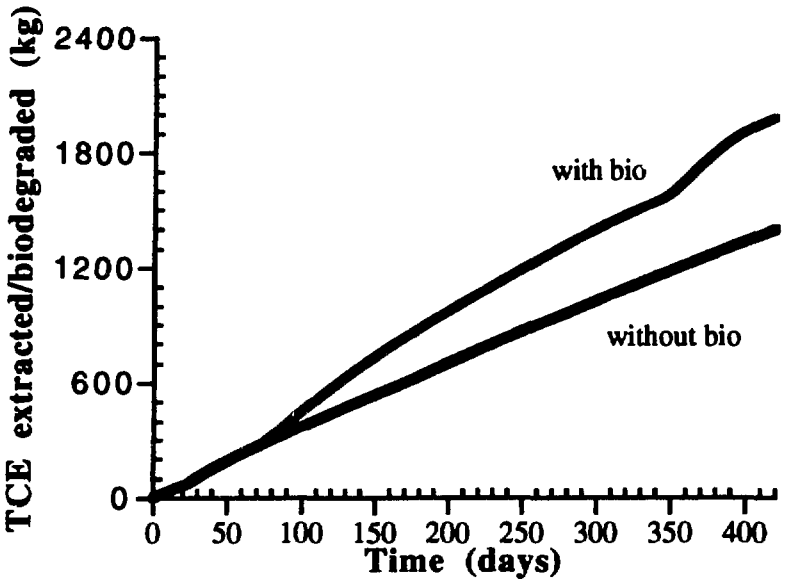

Fig. 5.4. TCE extracted/degraded vs. time for *in situ* bioremediation simulation and an identical simulation without microbial activity.

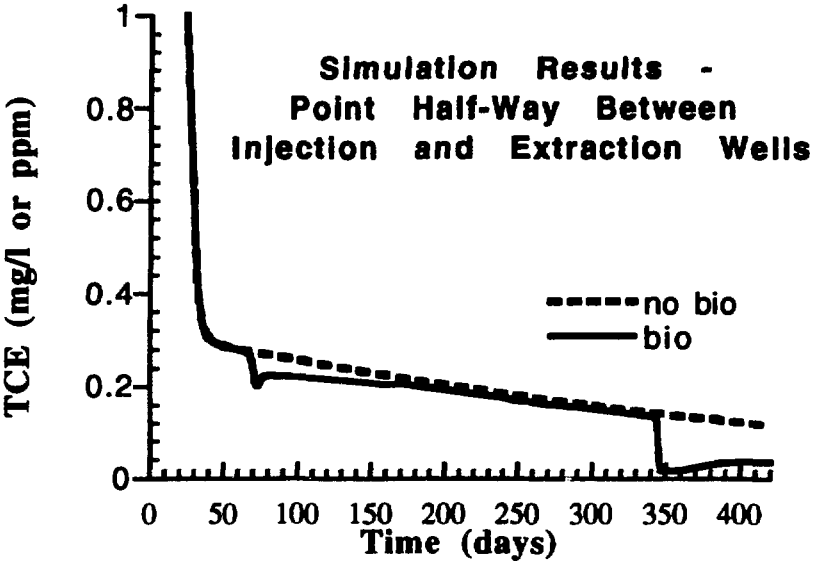

Fig. 5.5. Simulated TCE concentration vs.time profiles at a point half-way between injection and extraction wells for simulations with and without microbial activity.

APPENDIX A: Model Equations

TRAMP contains two sets of equations which are solved simultaneously. The first set includes the flow equations for unsaturated/saturated flow of air and water in heterogeneous, anisotropic porous media. These are time-dependent, three-dimensional equations which are solved using a finite difference, implicit time stepping algorithm. Material properties, such as porosity and permeability, can vary in space and the model allows considerable flexibility in boundary conditions and the location of injection/extraction wells. The flow equations are those included in TRACR3D (Travis and Birdsell 1991). Conservation of mass for the air phase is

$$\frac{\partial(\varepsilon\rho_g f)}{\partial t} + \nabla\cdot\left(\rho_g\vec{u}_g\right) = \varepsilon\dot{S}_g \tag{1}$$

and for the water phase is

$$\frac{\partial(\varepsilon\rho_w\sigma)}{\partial t} + \nabla\cdot\left(\rho_w\vec{u}_w\right) = \varepsilon\dot{S}_w. \tag{2}$$

The momenta conservation equations are approximated by Darcy's law (for low Reynolds number flows):

$$\vec{u}_i = -\frac{k_i}{\mu_i}\left(\nabla P_i + \rho_i\hat{g}\right) \tag{3}$$

where the subscript i refers to the air or water phase. The gas density is a function of pressure based on the ideal gas law. The numerical solution of the flow equations is not discussed here; the interested reader should consult Travis and Birdsell (1991).

The second set of equations in TRAMP includes six nonlinear, coupled, time-dependent transport equations, one each for oxygen, two nutrients, two substrates, and the microbes. Both anaerobic and aerobic conditions are included and Monod kinetics are assumed. Volatile constituents are assumed to partition between air and water phases according to Henry's Law. The relationship between the dissolved and sorbed phases is governed by an equilibrium sorption coefficient and a characteristic time scale such that transport between the phases can be modeled as instantaneous or time-dependent, as appropriate.

TRAMP is a general purpose code and therefore not all of its features may be needed at a specific site. The full equations are given here. Equation (4) is the conservation equation for the first substrate, substrate A. This equation states that the change in the amount of A in a given space for a specific (short) time period is equal to the amount of A consumed, the amount of A advected into or out of the space, and the amount of A diffused/dispersed into or out of the space. Consumption of A depends on the concentrations of oxygen, A, a nutrient, and bacteria in a straightforward Monod form. Anaerobic consumption of substrate A is inhibited by oxygen. In the Savannah River case, substrate A is methane.

(4)

$$\frac{\partial(\varepsilon\,(\sigma\rho_w + f\,H^A)[A]_w)}{\partial t} =$$

$$- \varepsilon\,\sigma\rho_w k_A [M]_w$$

$$* \left[\left(\frac{[A]_w}{K_A + [A]_w} \right) \left(\frac{[O_2]_w}{K_{O_2} + [O_2]_w} \right) \left(\frac{[N]_w}{K_N + [N]_w} \right) + J \left(\frac{[A]_w}{K'_A + [A]_w} \right) \left(\frac{[N]_w}{K'_N + [N]_w} \right) \left(\frac{I_{O_2}}{I_{O_2} + [O_2]_w} \right) \right]$$

$$- \nabla \cdot \left(\left(\vec{u_w} + H^A \vec{u_g} \right) [A]_w \right) + \nabla \cdot \left(\varepsilon\,(\sigma D_w^A + f\,H^A D_g^A) \nabla\,[A]_w \right) - (1 - \varepsilon)\,\rho_s \frac{d[A]_s}{dt}$$

where

$$\frac{d[A]_s}{dt} = \left(K_d^A [A]_w - [A]_s \right) / \tau^A$$

In the expression for $d[A]_s/dt$, a small value of τ means that the concentration of A inside soil grains is in equilibrium with the water phase concentration, with the partitioning determined by K_d. A large value of τ means there is a significant time lag for equilibration between liquid and solid phases. This would be reflected in a rapid drop in air phase concentration after a vacuum extraction well is turned on, followed by a slow increase after the vacuum is turned off. It is assumed in this model that τ is the diffusion time, given by particle radius squared divided by solid phase diffusivity.

The second equation (5) is the conservation equation for the second substrate, substrate B. In the Savannah River case, substrate A is TCE. Equation (5) states that the change in the amount of B in a given space for a specific time period is equal to the amount of B degraded by microbes, the amount of B advected into or out of the space and the amount of B diffused/dispersed into or out of the space. The rate of degradation of B depends on the microbe concentration and the concentrations of oxygen, nutrient and B. Substrate A can also affect substrate B's metabolism by inhibiting it at and above moderate concentrations. In a simulation of biodegradation of trichloroethylene by methanotropic bacteria, for example, A would be methane and B would be trichloroethylene. In a simulation of biodegradation of diesel oil, A would be the diesel oil and there would be no B.

(5)

$$\frac{\partial(\varepsilon\,(\sigma\rho_w + f\,H^B)[B]_w)}{\partial t} =$$

$$- \varepsilon\,\sigma\rho_w k_B [M]_w$$

$$* \left\{ \left(\frac{[B]_w}{[B]_w + K_B (1 + [A]_w / I_A)} \right) \left(\frac{[O_2]_w}{K_{O_2} + [O_2]_w} \right) \left(\frac{[N]_w}{K_N + [N]_w} \right) \right.$$

$$\left. + J \left(\frac{[B]_w}{[B]_w + K'_B (1 + [A]_w / I'_A)} \right) \left(\frac{[N]_w}{K'_N + [N]_w} \right) \left(\frac{I_{O_2}}{I_{O_2} + [O_2]_w} \right) \right\}$$

$$- \nabla \cdot \left(\left(\vec{u_w} + H^B \vec{u_g} \right) [B]_w \right) + \nabla \cdot \left(\varepsilon \left(\sigma D_w^B + f H^B D_g^B \right) \nabla [B]_w \right) - (1 - \varepsilon) \rho_s \frac{d[B]_s}{dt}$$

where

$$\frac{d[B]_s}{dt} = \left(K_d^B [B]_w - [B]_s \right) / \tau^B$$

The third equation (6) is the conservation equation for oxygen. Equation (6) states that the change in the amount of oxygen in a given space for a specific time period is equal to the amount of oxygen consumed, the amount of oxygen advected into or out of the space, and the amount of oxygen diffused/dispersed into or out of the space.

(6)

$$\frac{\partial \varepsilon \left(\sigma \rho_w + f H^{O2} \right) [O_2]_w}{\partial t} = - \varepsilon \sigma \rho_w [M]_w \left(\frac{[O_2]_w}{K_{O_2} + [O_2]_w} \right) \left(\frac{[N]_w}{K_N + [N]_w} \right)$$

$$* \left[(F_A)(k_A) \left(\frac{[A]_w}{K_A + [A]_w} \right) + (F_B)(k_B) \left(\frac{[B]_w}{[B]_w + K_B (1 + A_w / I_A)} \right) \right]$$

$$- \nabla \cdot \left(\left(\vec{u_w} + H^{O2} \vec{u_g} \right) [O_2]_w \right) + \nabla \cdot \left(\varepsilon \left(\sigma D_w^{O2} + f H^{O2} D_g^{O2} \right) \nabla [O_2]_w \right) - (1 - \varepsilon) \rho_s \frac{d[O_2]_s}{dt}$$

where

$$\frac{d[O_2]_s}{dt} = \left(K_d^{O2} [O_2]_w - [O_2]_s \right) / \tau^{O2}$$

The fourth equation (7) is the conservation equation for a nutrient (e.g., phosphate or nitrate). Equation (7) states that the change in the amount of nutrient in a given space for a specific time period is equal to the amount of nutrient consumed, the amount of nutrient advected into or out of the space, the amount of nutrient dispersed into or out of the space and the amount of nutrient returned to the system from dead and decaying microbes. An identical fifth equation allows for a second nutrient.

(7)

$$\frac{\partial \left[\varepsilon \left(\sigma \rho_w + f H^N \right) [N]_w \right]}{\partial t} =$$

$$- \varepsilon \sigma \rho_w F_N k_M [M]_w$$

$$* \left\{ \left(\frac{[O_2]_w}{K_{O_2} + [O_2]_w} \right) \left(\frac{[N]_w}{K_N + [N]_w} \right) \left[\left(k_A Y_A \frac{[A]_w}{K_A + [A]_w} \right) + \left(k_B \frac{\max(0., Y_B)[B]_w}{K_B (1 + [A]_w / I_A) + [B]_w} \right) \right] \right.$$

$$\left. + J \left(\frac{I_{O_2}}{I_{O_2} + [O_2]_w} \right) \left(\frac{[N]_w}{K'_N + [N]_w} \right) \left[\left(k_A Y_A \frac{[A]_w}{K'_A + [A]_w} \right) + \left(k_B \frac{\max(0., Y_B)[B]_w}{K'_B (1 + [A]_w / I'_A) + [B]_w} \right) \right] \right\}$$

$$- \nabla \cdot \left(\vec{u_w} + H^N \vec{u_g} \right) [N]_w + \nabla \cdot \left(\varepsilon \left(\sigma D_w^N + f H^N D_g^N \right) [N]_w \right)$$

$$+\left[k_d\left(\frac{[O_2]_w}{I_{O_2}+[O_2]_w}\right)+k_d'\left(\frac{I_{O_2}}{I_{O_2}+[O_2]_w}\right)\right][M]_w X_{dM}$$

$$-(1-\varepsilon)\rho_S\frac{d[N]_S}{dt}$$

where

$$\frac{d[N]_S}{dt}=\left(K_d^N[N]_w-[N]_S\right)/\tau^N$$

The final equation, Eq. (8), describes the conservation of bacteria. The terms on the right hand side represent, respectively, growth due to degradation of substrates A and B, loss due to microbial death, and growth based on consumption of any naturally occurring organic material in the soil. The bacteria are assumed to be immobile so there are no advection and dispersion terms. All of the microbial activity takes place in the liquid phase. It is also assumed that the constituents in the water and biofilms are well-mixed so that there is no gradient and no mass transfer delay within the fluid layer. The consumption terms depending on B in Eqs. (7) and (8) allow for the possibility that some bacteria may actually gain energy from breakdown of B. However, if B is toxic or inert, the term will disappear.

(8)

$$\frac{\partial[M]_w}{\partial t}=$$

$$k_M[M]_w\left\{\left(\left(\frac{k_A Y_A[A]_w}{K_A+[A]_w}\right)+\left(\frac{k_B \max(0.,Y_B[B]_w}{K_B(1+[A]_w/I_A)+[B]_w}\right)\right)\left(\frac{[N]_w}{K_N+[N]_w}\right)\left(\frac{[O_2]_w}{K_{O_2}+[O_2]_w}\right)\right.$$

$$\left.+J\left(\left(\frac{k_A Y_A[A]_w}{K_A'+[A]_w}\right)+\left(\frac{k_B \max(0.,Y_B[B]_w}{K_B'(1+[A]_w/I_A')+[B]_w}\right)\right)\left(\frac{[N]_w}{K_N'+[N]_w}\right)\left(\frac{I_{O_2}}{I_{O_2}+[O_2]_w}\right)\right\}$$

$$-\left[k_d\left(\frac{[O_2]_w}{I_{O_2}+[O_2]_w}\right)+k_d'\left(\frac{I_{O_2}}{I_{O_2}+[O_2]_w}\right)\right][M]_w+k_d[NOC]$$

The symbols used in Eqs (1)-(8) are defined in Table A.1. Values for the various biokinetic parameters necessary for these simulations are assumed to be constant in time and correspond to a temperature of 20°C.

Table A.1. Symbols

'	anaerobic parameters
ε	porosity
k	permeability
ρ	density
μ	viscosity
σ	water phase saturation
τ	characteristic time scale for diffusion of species into/out of soil particles $= d^2/4D_s$ where d is the particle diameter and D_s is the diffusion coefficient in the solid phase, assumed to be 10^{-10} cm^2/s
A	substrate A (methane)
B	substrate B (TCE)
B_R^i	nonlinear term for species i representing biological metabolic reactions
$[C]_i$	concentration of species i in liquid phase, g/cm^3
D	dispersivity/diffusivity
F	the mass ratios of oxygen consumed per mass of substrate/nutrient
f	air phase saturation
g	gas phase
$\hat{g}$	gravity acceleration
H	Henry's Law coefficient
I	inhibition half saturation concentration (the substrate/nutrient concentration at which the maximum utilization rate is reduced by half)
i	refers to one of the species
J	ratio of anaerobic to aerobic utilization rates
K	half saturation concentration (the substrate/nutrient concentration at which the utilization rate is half the maximum)
k	maximum rate of substrate utilization
k_c	background growth rate of microbes
K_d	equilibrium sorption coefficient
k_d	death rate of microbes
L_i	differential operator for the ith species
M	microbes (bacteria)
N	nutrient
NOC	natural organic carbon
O_2	oxygen
R	factor corresponding to nonequilibrium sorption effect
s	sorbed phase
$\dot{S}$	mass source or sink
t	time
$\vec{u}$	velocity vector
w	liquid water phase
X_{dM}	fraction of dead microbes converted to available nutrients
Y	the microbial yield per unit of substrate consumed

APPENDIX B: Brief Summary of *In Situ* Air Stripping Performance Assessment

A brief summary of a performance assessment of the *in situ* air stripping demonstration at the SRID site, based on modeling studies, is given below. Details are contained in Robinson et al. (1994) and Birdsell et al. (1994).

Major conclusions regarding the *in situ* air stripping technology demonstrated at Savannah River include the following:

- The TCE concentration at the extraction well versus time can be simulated very well using a relatively simple model with a dual porosity formulation. The model assumes a mass transfer limitation between liquid-phase TCE held up in clay lenses and the moving air, which travels mainly in the surrounding sandy zones of higher permeability.
- Cyclic operation of the system may offer substantial cost savings for only a marginal performance cost. For example, operating the *in situ* air stripping system on a 30-day-on, 30-day-off schedule rather than a continuous basis results in only about a 35% decrease in total TCE removal. Similarly, operating the system at lower flow rates may offer substantial cost savings for only a marginal performance cost. For example, an increase in flow rate by a factor of four resulted in only a 26% increase in total TCE removal.
- The injection of heated air through the lower well is unlikely to result in increased TCE removal. This is because only a small region is heated at any one time and as soon as air travels from a heated region to one at ambient temperature, any "extra" TCE in the air phase will redissolve.
- Aligning the injection and extraction wells at any particular angle to one another is probably not necessary. Heterogeneities in the medium are likely to be the dominant factor in governing the spreading of air in the saturated zone and for any reasonable configuration, it is very unlikely that TCE stripped from the saturated zone would not be captured by the extraction well. The injection well should be directly aligned with the major axis of the plume in the horizontal plane for the greatest likelihood of adequate air sweep through the plume.
- A system consisting of a horizontal air injection well and vertical extraction well(s) in the vadose zone with surface capping may be an optimal *in situ* air stripping system, provided access is not an issue and capping is possible.
- The TCE removal curve is very asymptotic.
- The main characteristic in assessing the performance of this technology at another site is the heterogeneity of the site. The more heterogeneous the site, the longer it will take to remediate the site (assuming contaminants are in the lower permeability zones).
- Model results suggest that replacing the lower air injection well with a groundwater pumping well (also horizontal) results in more TCE being extracted from the groundwater, but the amount of TCE below the water table that is removed in both cases is small.

Major conclusions regarding vapor extraction wells, in general, include the following:

- In an accessible, homogeneous medium, a single horizontal, vapor extraction well outperforms (i.e., achieves a lower level of residual contamination in a shorter amount of time) a single vertical, vapor extraction well at a capped site only for a long linear plume. Here, "long" means that the plume extends beyond the radius of influence of the vertical well. However, the radius of influence of a vertical well can often be increased so that it "beats" the horizontal well by increasing its extraction rate. Also, two vertical wells with site capping may outperform a single horizontal well if the plume extends beyond the

radius of influence of the single vertical well. A horizontal well often outperforms a vertical well in the absence of site capping.

- For heterogeneous systems, site-specific simulations are required to determine the most effective remediation strategy for vapor extraction. However, we believe that the above conclusions are generally true for an accessible, heterogeneous medium (e.g., low permeability clay lenses in a relatively high permeability sand) as well. (Horizontal wells may provide an advantage for remediating areas with contaminant located in vertical fractures by intercepting a greater number of fractures than possible with a vertical well, but this case was not considered here.)
- For maximum removal efficiencies during vapor extraction the following guidelines are suggested. Surface capping should be used with vertical extraction wells. Both horizontal and vertical wells should be screened over the entire length of the plume. A horizontal well should be placed at the lower edge of the plume and aligned with the plume's major axis in the horizontal plane. A vertical well should be placed in the center of the plume.

REFERENCES

Andrews, G. F. (1994), Biodegradation/Activity, *Idaho National Engineering Laboraotry, draft report..*

Andrews, G. F., F. C. Colwell, K. Dinerstein and S. Hansen (1991), The Kinetics of TCE Degradation in a Soil Environment, *Presentation At American Institute of Chemical Engineers Annual Meeting*, Los Angeles, CA.

Bear, J. (1979), *Hydraulics of Groundwater*, Mcgraw-Hill International Book Co., New York.

Bentley, H. (1990), *Private Communication*, Hydrogeochem, Inc., Tucson AZ.

Bentley, H. and B. J. Travis (1992), Modeling In-Situ Biodegradation in Unsaturated and Saturated Soils, *(Abstract),* In: *Proceedings of The Symposium On Soil Venting (EPA/600/R-92/174).*

Birdsell, K. H., N. D. Rosenberg and K. M. Edlund (1994), The Performance of Horizontal Versus Vertical Vapor Extraction Wells, *Los Alamos National Laboratory report LA-12783-MS.*

Celia, M. A., J. S. Kindred and I. Herrera (1989), Contaminant Transport and Biodegradation 1. A Numerical Model for Reactive Transport in Porous Media, *Water Resources Research 25*, 1141-1148.

Eddy, C. A., B. B. Looney, J. M. Dougherty, T. C. Hazen and D. S. Kaback (1991), Characterization of the Geology, Geochemistry, Hydrology and Microbiology of the In Situ Air Stripping Demonstration Site at the Savannah River Site, *Westinghouse Savannah River Company report WSRC-Rd-91-21.*

Eddy Dilek, C. A., B. B. Looney, T. C. Hazen, R. L. Nichols, D. S. Kaback and J. L. Simmons (1993), Post-Test Evaluation of the Geology, Geochemistry, Hydrology and Microbiology of the In Situ Air Stripping Demonstration Site at the Savannah River Site, *Westinghouse Savannah River Company report WSRD-RD-93-369.*

Hazen, T. C. (1992a), Test Plan for In Situ Bioremediation Demonstration of the Savannah River Integrated Project DOE/OTD TTP No. SR 0566-01, *Westinghouse Savannah River Company report WSRC-RD-91-23.*

Hazen, T. C. (1992b), Data for In Situ Bioremediation Demonstration of Savannah River Integrated Demonstration Project DOE/OTD, *Westinghouse Savannah River Company report October 26, 1993.*

Kinzelbach, W., W. Shäfer and J. Herzer (1991), Numerical Modeling of Natural and Enhanced Denitrification Processes in Aquifers, *Water Resources Research 27*, 1123-1135.

Looney, B. B., T. C. Hazen, D. S. Kaback and C. A. Eddy (1991), Full Scale Field Test of the In Situ Air Stripping Process at the Savannah River Integrated Demonstration Test Site, *Westinghouse Savannah River Company report WRSC-RD-91-22.*

MacQuarrie, K. T. B., E. A. Sudicky and E. O. Frind (1990), Simulation of Biodegradable Organic Contaminants in Groundwater 1: Numerical Formulation in Principal Directions, *Water Resources Research 26*, 207-222.

Molz, F. J., M. A. Widdowson and L. D. Benefield (1986), Simulation of Microbial Growth Dynamics Coupled to Nutrient and Oxygen Transport in Porous Media, *Water Resources Research 22*, 1207-1216.

Oreskes, N., K. Shrader-Frechette, and K. Belitz (1994), Verification, Validation, and Confirmation of Numerical Models in the Earth Sciences, *Science, 263*, 641-646.

Pruess, K. (1993), Analysis of Flow Processes During TCE Infiltration in Heterogeneous Soils at the Savannah River Site, Aiken, South Carolina, *Lawrence Berkeley Laboratory report LBL-32418.*

Rifai, H. S. and P. B. Bedient (1990), Comparison of Biodegradation Kinetics with an Instantaneous Reaction Model for Groundwater, *Water Resources Research 26*, 637-645.

Roberts, P. V., G. D. Hopkins, D. M. Mackay, and L. Semprini (1990), A Field Evaluation of In-Situ Biodegradation of Chlorinated Ethenes: Part 1, Methodology and Field Site Characterization, *Groundwater 28*, 591-604.

Robinson, B. A., N. D. Rosenberg, G. A. Zyvoloski, and H. Viswanathan (1994), Simulations of *In Situ* Air Stripping Demonstration at Savannah River, *Los Alamos National Laboratory report LA-12781-MS.*

Semprini, L., and McCarty, P. L. (1991), Comparison Between Model Simulations and Field Results for In Situ Biorestoration of Chlorinated Aliphatics: Part 1. Biostimulation of Methanotrophic Bacteria, *Groundwater 29,* 365-374.

Semprini, L., G. D. Hopkins, P. V. Roberts, D. Grbic-Galic, and P. L. McCarty (1991), A Field Evaluation of In-Situ Biodegradation of Chlorinated Ethenes: Part 3. Studies of Competitive Inhibition, *Groundwater 29*, 239-250.

Semprini, L., P. V. Roberts, G. D. Hopkins and P. L. McCarty (1990), A Field Evaluation of In-Situ Biodegradation of Chlorinated Ethenes: Part 2. Results of Biostimulation and Biotransformation Experiments, *Groundwater 28*, 715-727.

Travis, B. J. (1984), TRACR3D: A Model of Flow and Transport In Porous/Fractured Media, *Los Alamos National Laboratory report LA-9667-MS.*

Travis, B. J. (1993), TRAMP (TRACR3D With Microbial Processes): A Numerical Code for *In Situ* Bioremediation Simulations, *Los Alamos National Laboratory document LA-UR-93-479.*

Travis, B. J., N. D. Rosenberg and K. H. Birdsell (1993), Preliminary Simulations of *In Situ* Bioremediation at The Savannah River Site, *Los Alamos National Laboratory document LA-UR-93-480.*

Travis, B. J. and K. H. Birdsell (1991), TRACR3D: A Model of Flow and Transport in Porous Media: Model Description and User's Manual, *Los Alamos National Laboratory document LA-UR-11798-M.*

Vlachopoulos and Kitinidis (1994), A Numerical Model of Air Flow During Sparging, *Department of Civil Engineering, Stanford University, draft report,* February 11, 1994.

Wheeler, M. F., K. R. Roberson and A. Chilakapati (1992), Three-Dimensional Bioremediation Modeling on Heterogeneous Porous Media, In: *Computational Methods In Water Resources IX* Volume 2 (Ed: T. F. Russell, R. E. Ewing, C. A. Brebbia, W. G. Gray and G. F. Pinder), Mathematical Modeling in Water Resources, Computational Mechanics Publications, Boston.

Widdowson, M. A., F. J. Molz and L. D. Benefield (1988), A Numerical Transport Model for Oxygen- and Nitrate-Based Respiration Linked to Substrate and Nutrient Availability in Porous Media, *Water Resources Research 24,* 1553-1565.